Untargeted analysis E-noses and FTIR

Electronic nose (E-nose)

- Electronic noses are engenireed to mimic the mammalyan olfactory sistem
- Instrumentent designed to allow detection and classification of aroma mixtures
- Refers to the capability of reproducyng human senses using sensor arrays and pattern recognition system

✓ *cosmetic industry control*

✓ *food quality and safety control*

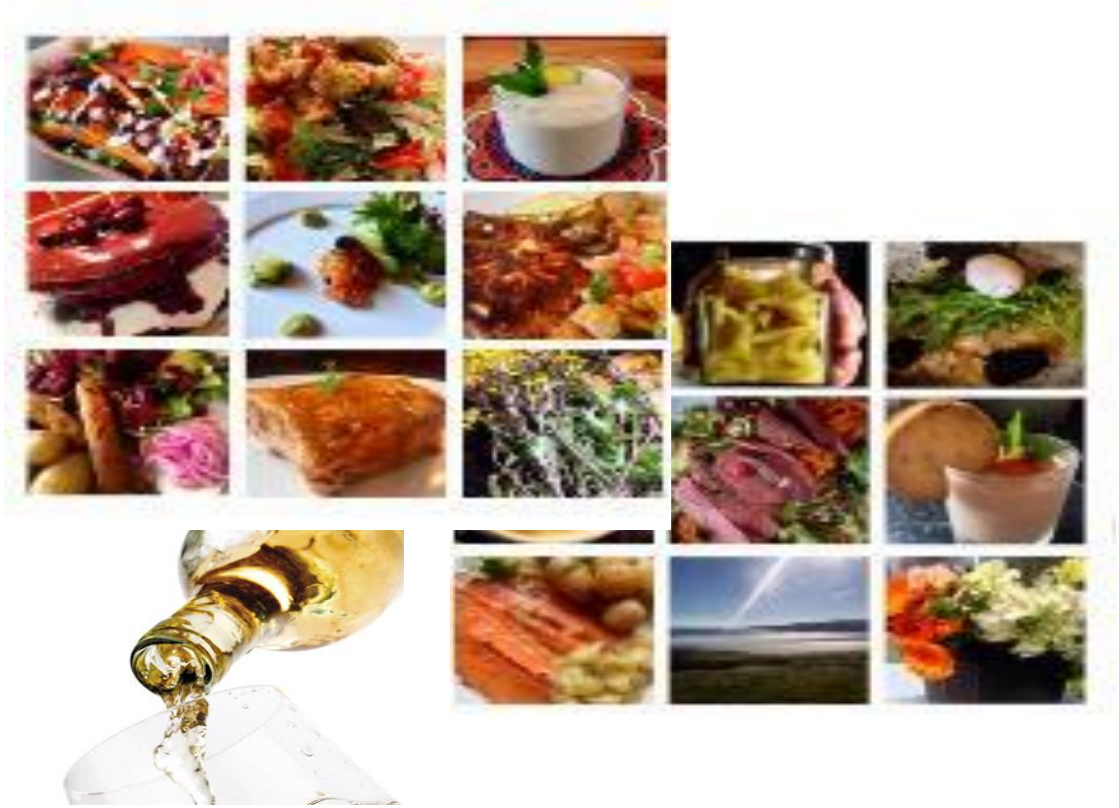

✓ *environmental monitoring for air quality control*

An electronic nose can now diagnose cancerous tumors. A new research have designed an electronic nose to help diagnose malignant mesothelioma early on. This nose can detect the presence of the tumor with a breath test. Malignant mesothelioma is an uncommon, usually fatal, cancerous tumour of the lining of the lung and chest cavity or lining of the abdomen (peritoneum) caused by long-term asbestos exposure. The device was designed to distinguish between benign and malignant disease and to detect the disease early. “If you catch it earlier, your chances of actually giving people the right treatment to stop it spreading are actually better,” said team leader, Deborah Yates. “We tried to exclude the other asbestos diseases because it’s very important from a patient’s point of view that you don’t pick up something that is a benign asbestos disease, so that you don’t diagnose them with something that’s not actually a problem,” added Yates.

https://www.thehealthsite.com/news/electronic-nose-helps-locate-deadly-tumour/

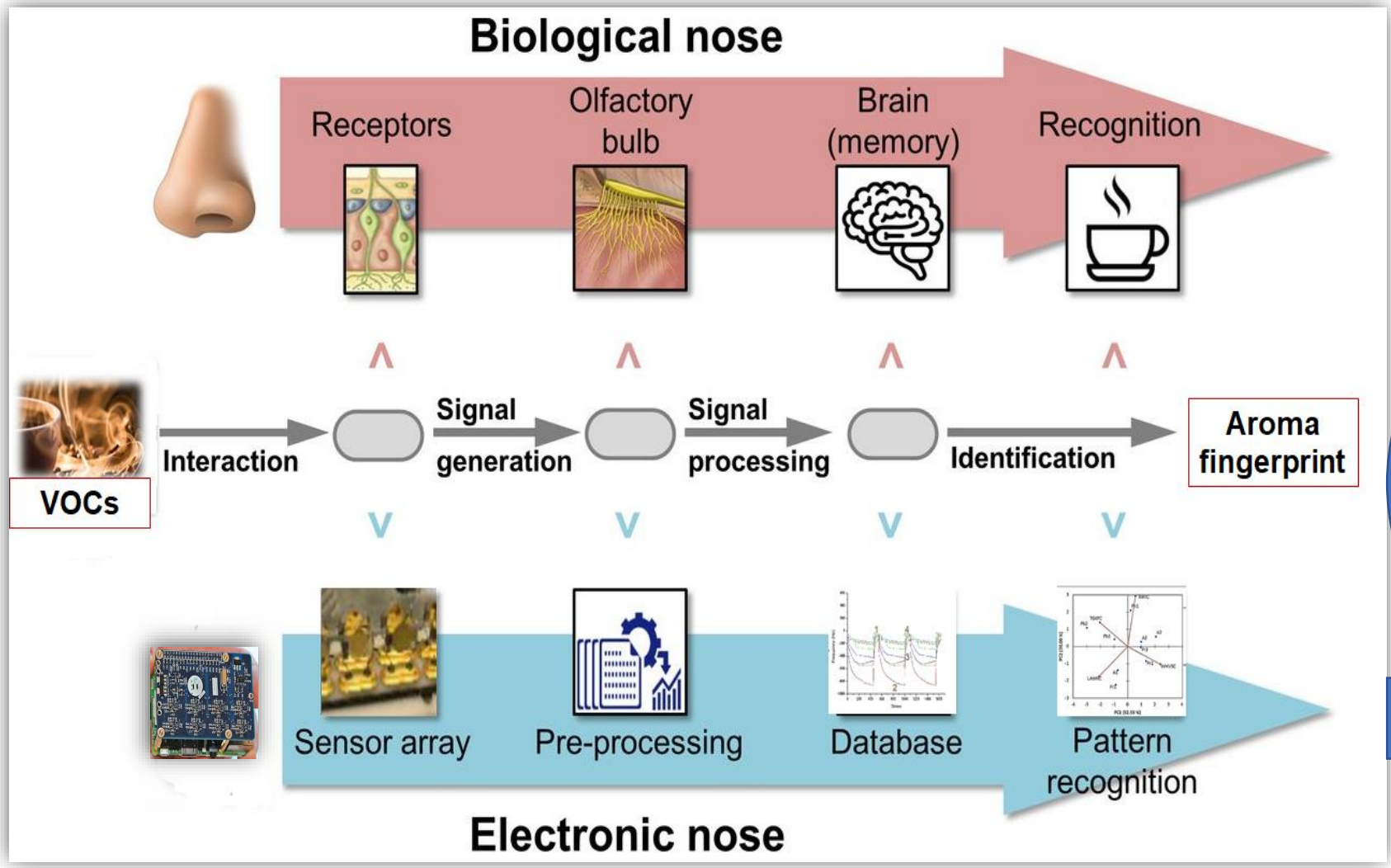

'An electronic nose is an instrument, which comprises an array of electronic chemical sensors with partial specificity and an appropriate pattern-recognition system, capable of recognizing simple or complex odors' [1]

[1] Gardner, Julian W., and Philip N. Bartlett. "A brief history of electronic noses." *Sensors and Actuators B: Chemical* 18.1-3 (1994): 210-211.

….Different type of transducer for gas sensing….

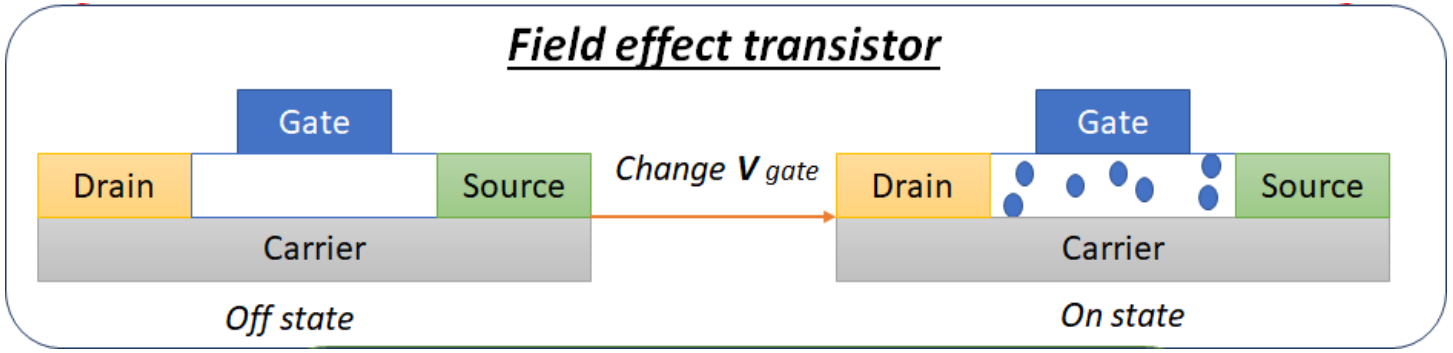

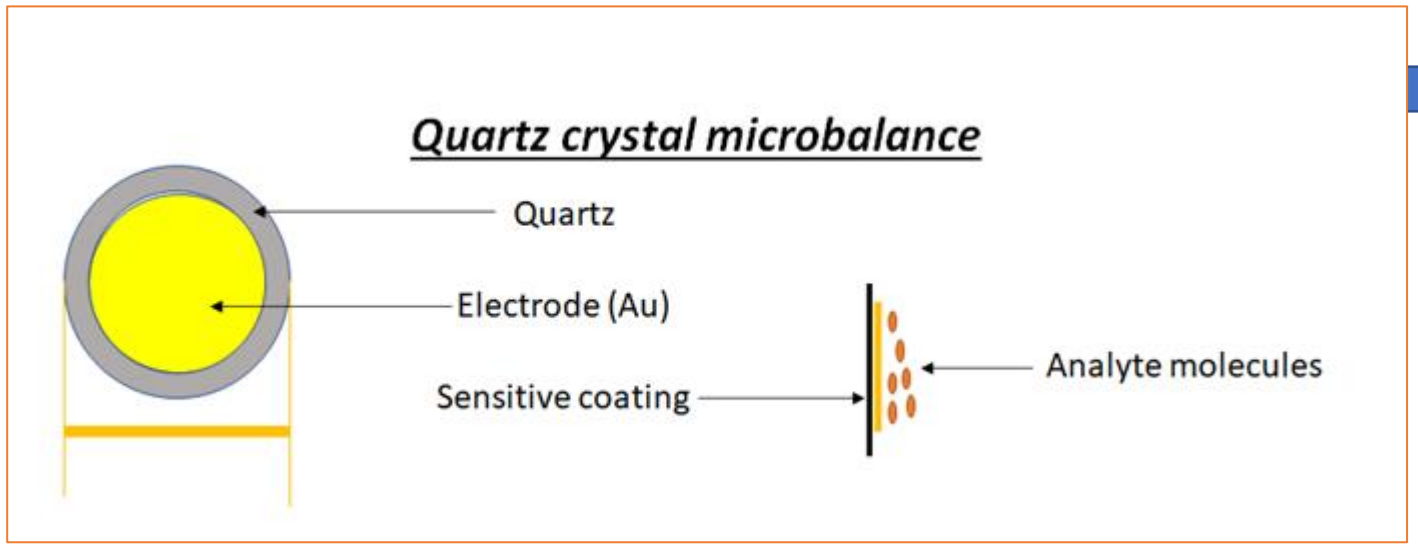

- ✓ *low costs*
- ✓ *easy realization*
- ✓ *ability to work in real-time*
- ✓ *short analysis times*

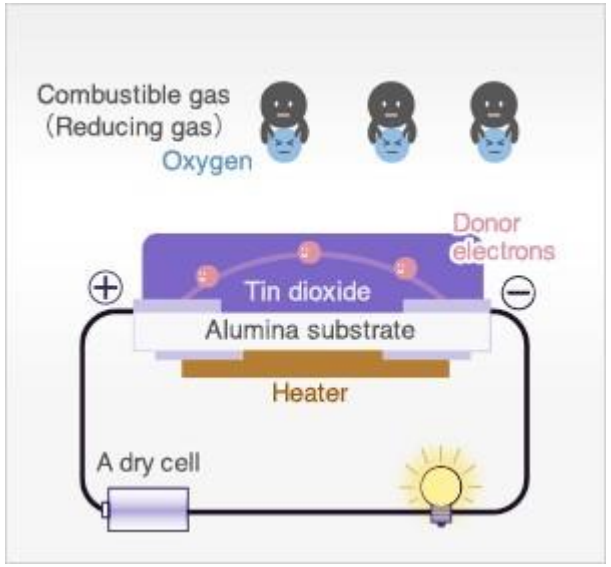

MOS SENSORS

Metal oxide semiconductors

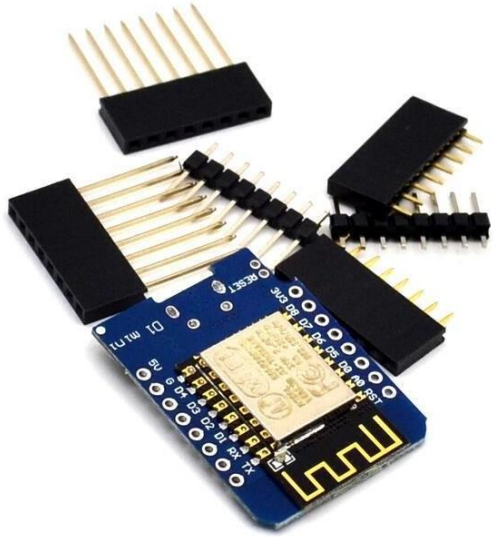

Constituted by three main parts:

- Ceramic substrate
- Heating wire or thermistor
- Semiconducting metal oxides film (Zn, Co, etc.)

They measure conductivity changes onto the surface of the sensors induced by gases. Sensitive to combustion gases (hydrocarbons, NO, CO). Work at 300-400°C. An exchange between the gas and the oxygen on the film causes a change in resistance dependent on the adsorbed gas.

MOSFET SENSORS

Field effect metal oxides transistors

Made by 3 parts:

- Semiconducting Silicon
- Insulating silica layer
- Catalytic metal (Pt, Pd, etc.)

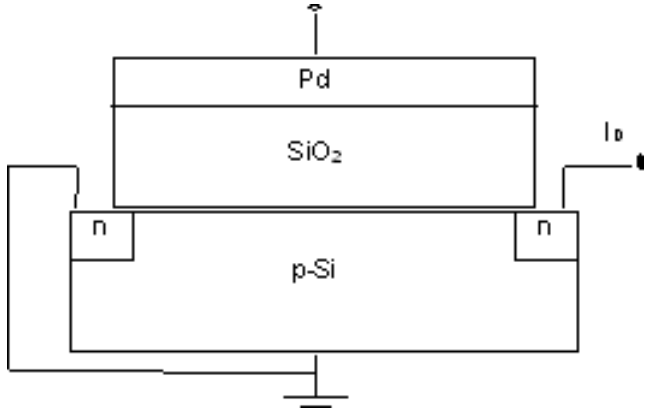

Work as a transistor at applied potential at 140-170°C. Sensitive to compounds containing hydrogen (amines, aldehydes, esters, chetons, aromatics ed alcohols). Whwn a polar molecules interacts with the metal the electric field is modified and a change in current occurs. The device output is the voltage necessary to have the current back at the initial value.

Piezoelectric System
Electronic nose

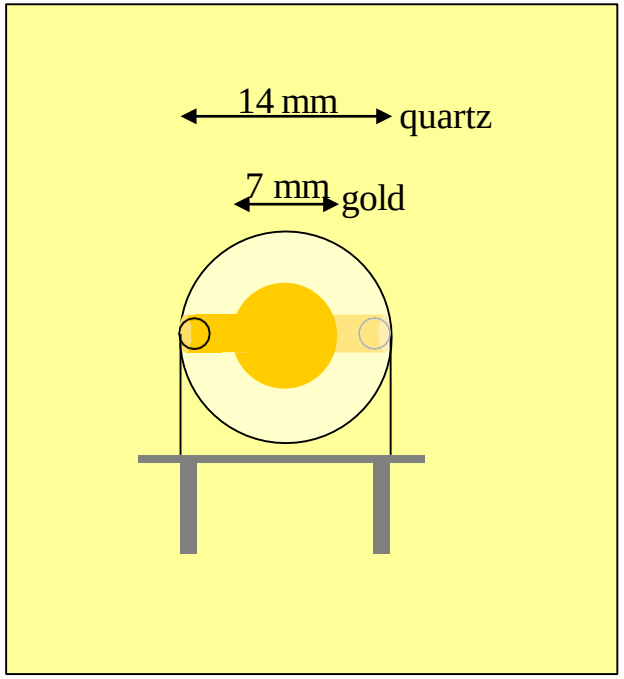

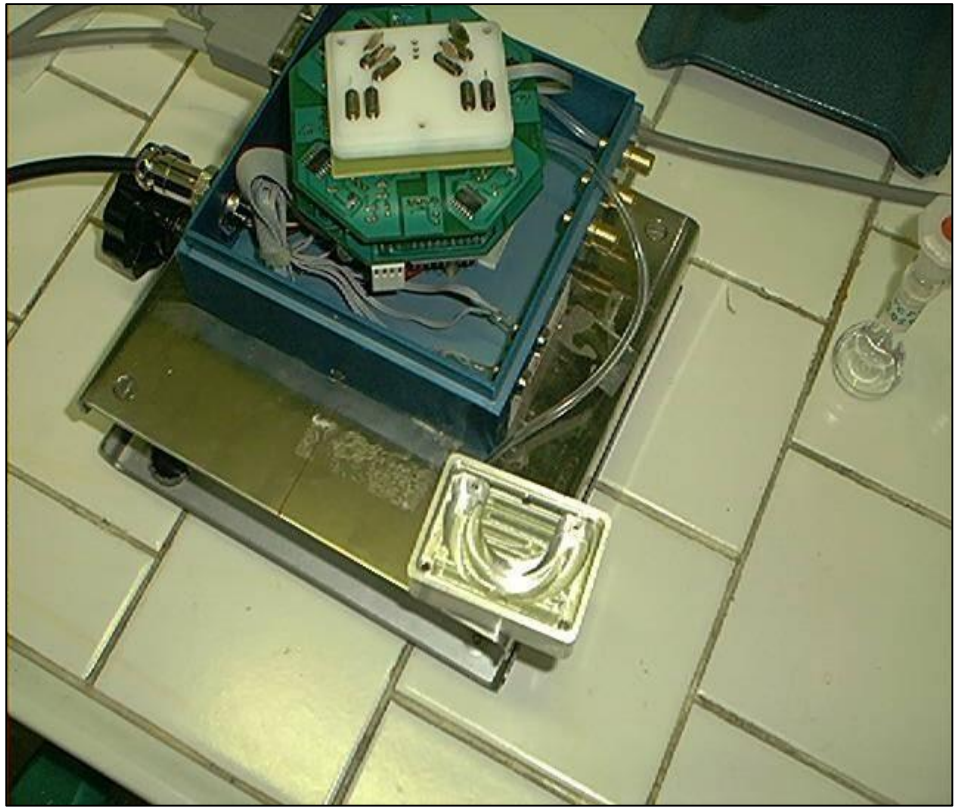

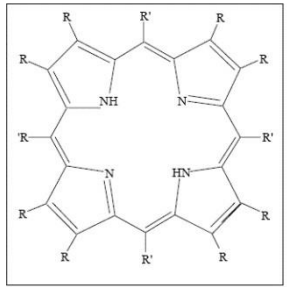

Butiloxy Tetra Phenyl Porphyrin

Cu
Co
Zn
Mn
Fe
Sn
Ru
Cr

Measurement system

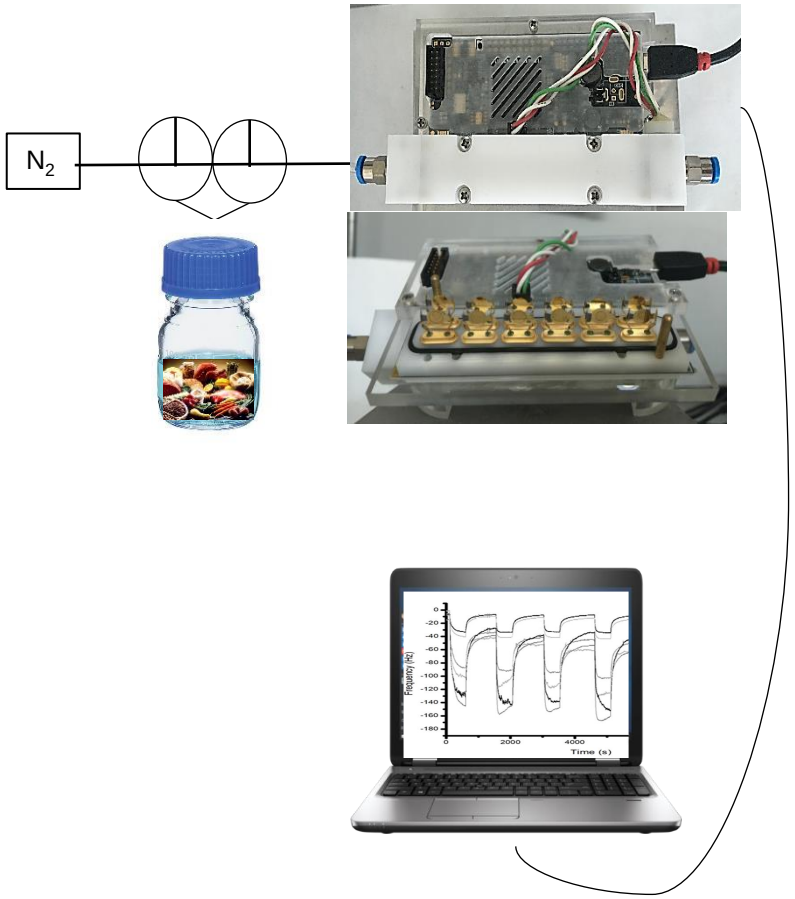

1.Start

2.Decrease

3.Equilibration

4.Baseline

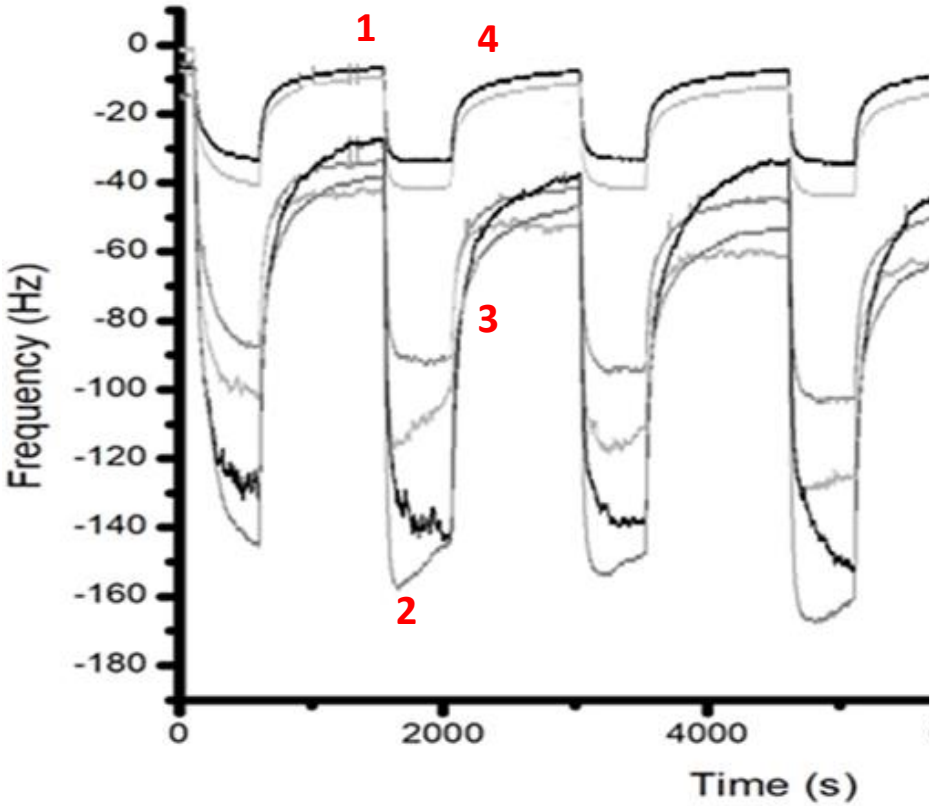

Frequency signals recorded with ZnONPs-peptides testing food

Electronic nose

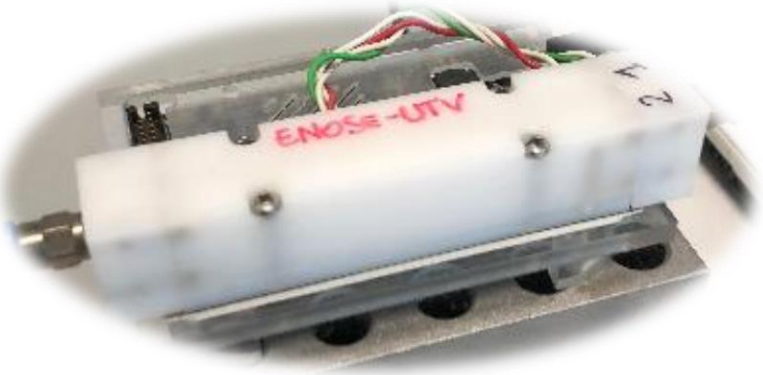

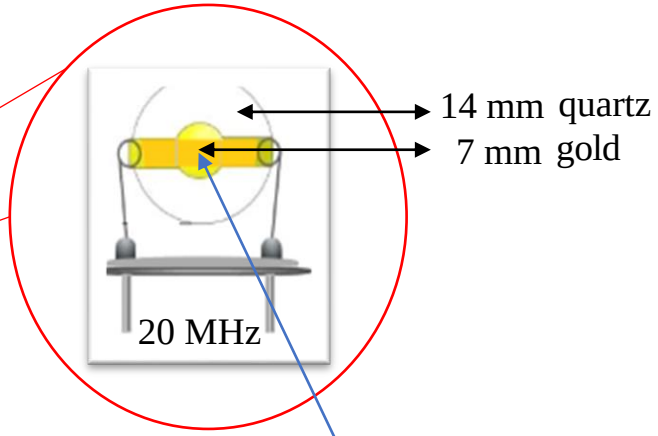

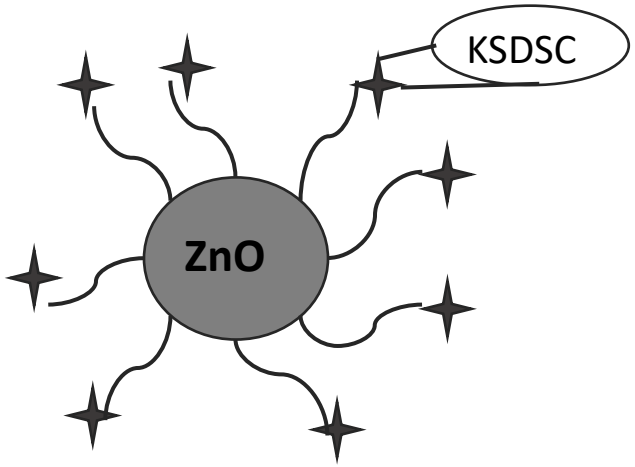

ZnONPs-Peptides

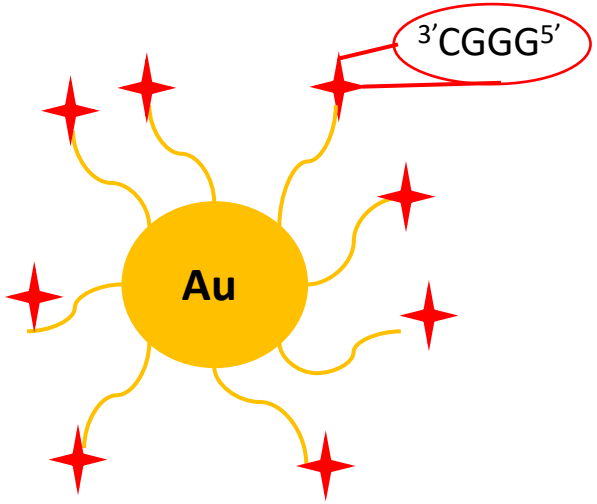

AuNPs-hpDNA

AuNPs-hpDNA

ZnONPs-Peptides

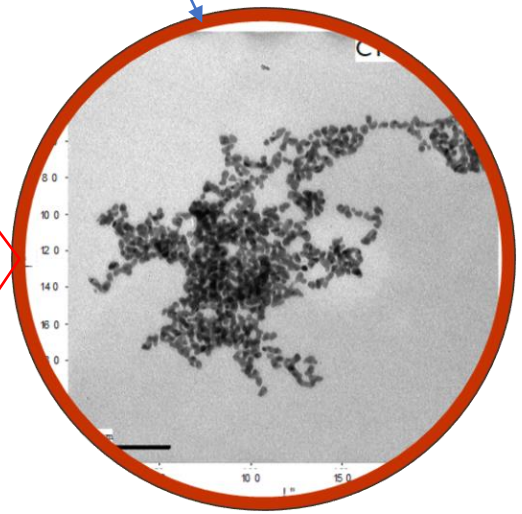

UNITE

Electronic nose sensor arrays

GNP-Peptide based

- **AuNP-Glutathione**
- **AuNP-Cys-Gly**
- **AuNP-Cys**
- **AuNP-Thioglicolic Acid**
- **AuNP-Cys-Arg-Gln-Val-Phe**
- **AuNP-Cys-Ile-His-Asn-Pro**
- **AuNP-Cys-Ile-Gln-Pro-Val**
- **AuNP**

Porphyrin based

- **Cu-Buti-TPP**
- **Co-Buti-TPP**
- **Zn-Buti-TPP**
- **Mn-Buti-TPP**
- **Fe-Buti-TPP**
- **Sn-Buti-TPP**
- **H_2-Buti-TPP**
- **Mg-Buti-TPP**

UNITE

- **Temperature: 40°C**
- **Equilibration time: 10 min**
- **15g in 100 mL lab bottle grated and melted**
- **N_2 = 4 L/h**

Standard Samples
VS
Off-flavoured samples

PLS-DA analysis

Off-Flavour	Process
3-methylbutanal	**Fermentation volatiles**
Phenylacetaldehyde	
Acetic Acid	**Conching process**
Tetramethylpyrazine	**Roasting Process**
2-acetylpyrrole	
2-nonenal	**Fat related (oxidation)**
2,4-decadienal (t,t)	

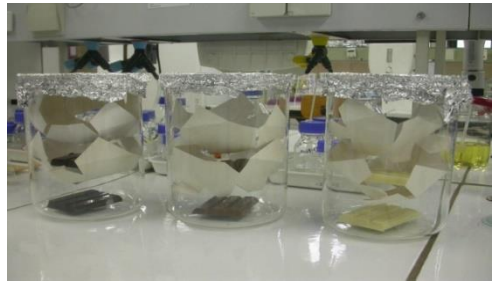

Off-flavours were preliminarily added in the cocoa butter to achieve the concentration of 125 ppm. One tea spoon of contaminated cocoa butter was then added to 400 g of chocolate to obtain an estimated final concentration in the sample of ~ 6ppm.

Real samples

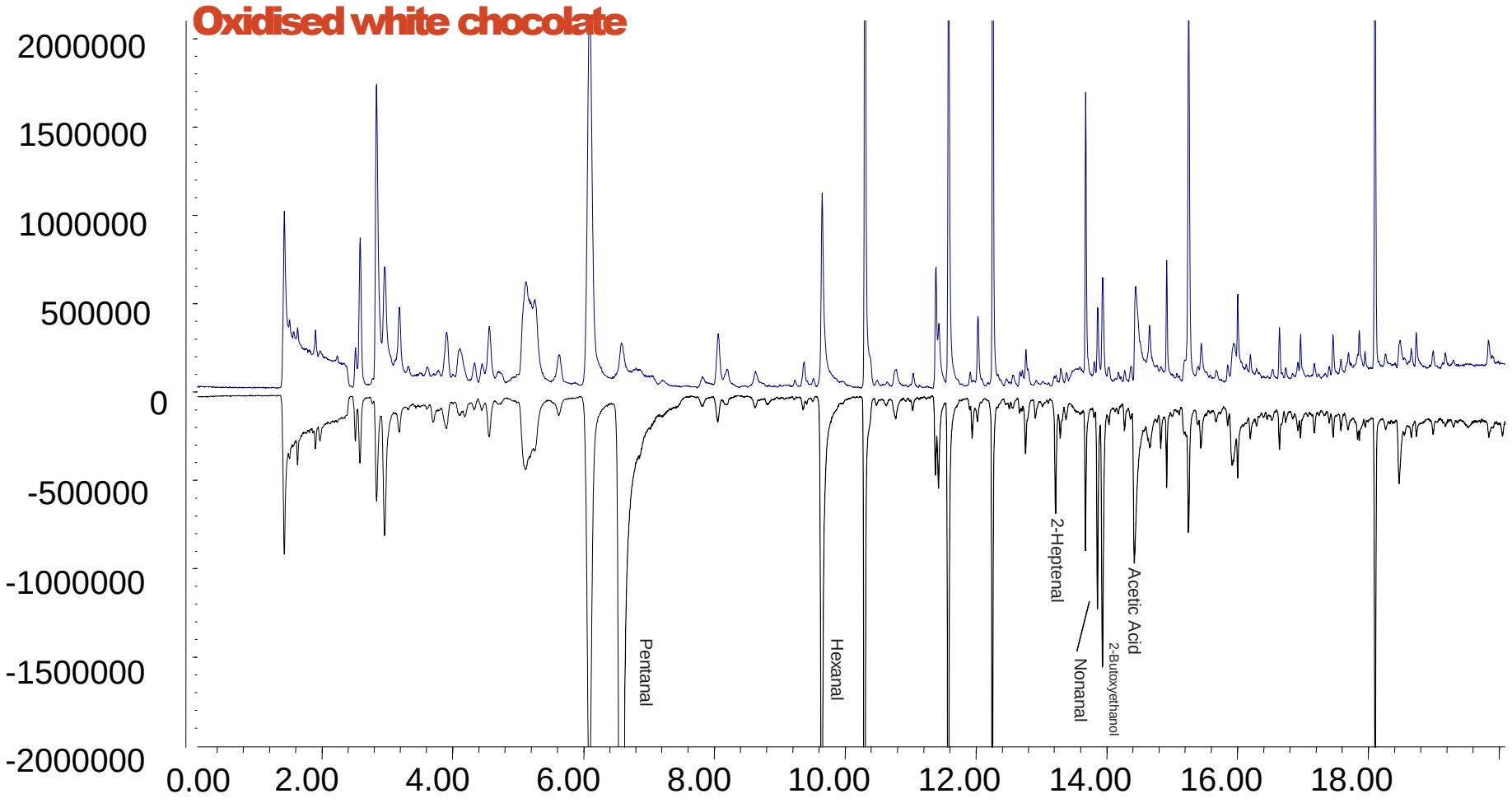

Dark Chocolate

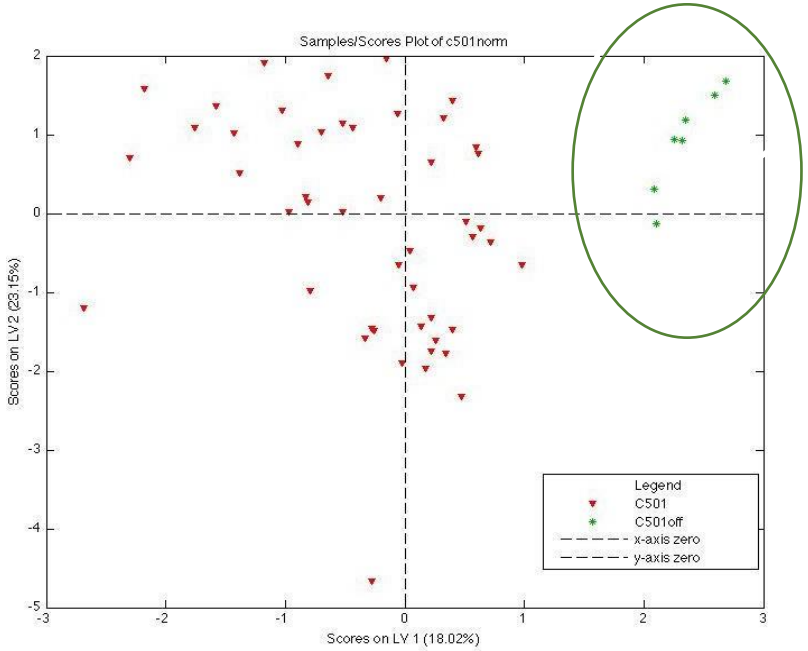

White Chocolate

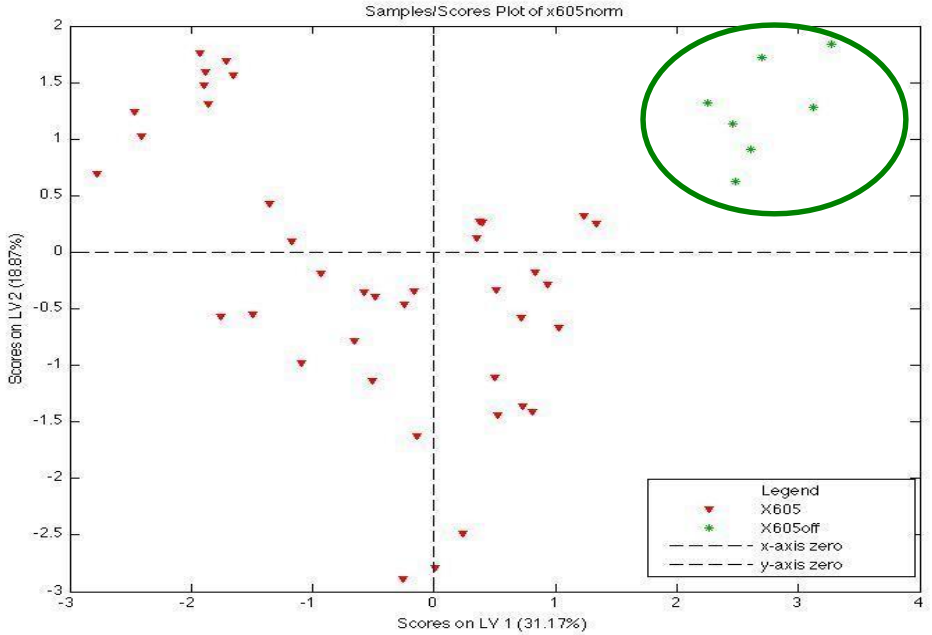

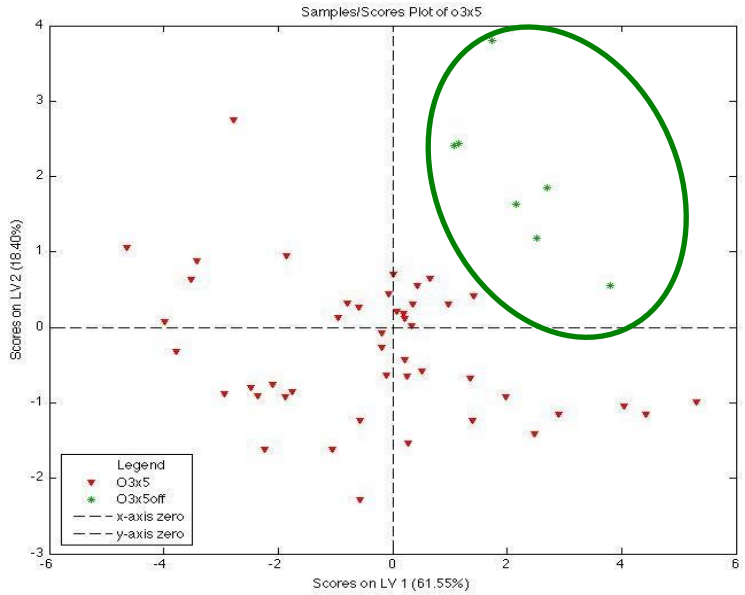

Milk Chocolate

UNITE

AuNP-Peptide vs. Porphyrin PLS-DA analysis

GNP-Peptide based

	Regular	Off Flavours	% Correct
Regular	48	0	100
Off flavours	0	7	100

Tot. Correct:

	Regular	Off Flavours	% Correct
Regular	39	0	100
Off flavours	0	7	100

Tot. Correct:

	Regular	Off Flavours	% Correct
Regular	51	1	98
Off flavours	0	7	100

Tot. Correct:

Porphyrin based

	Regular	Off Flavours	% Correct
Regular	14	1	93
Off flavours	1	9	90

Tot. Correct:

	Regular	Off Flavours	% Correct
Regular	13	1	92
Off flavours	4	8	67

Tot. Correct:

	Regular	Off Flavours	% Correct
Regular	15	1	94
Off flavours	4	8	67

Tot. Correct:

D. Compagnone, M. Faieta, D. Pizzoni, C. Di Natale, et al *Sensors and Actuators B*, 207, 1114, 2015.

Virtual screening Peptides

6 Peptides studied
(KSDSC, WHVSC, LGFDC, IHRIC, LAWHC, TGKFC)

VS

14 volatile compounds
(different chemical classes, shapes, dimensions, hydrophobicity)

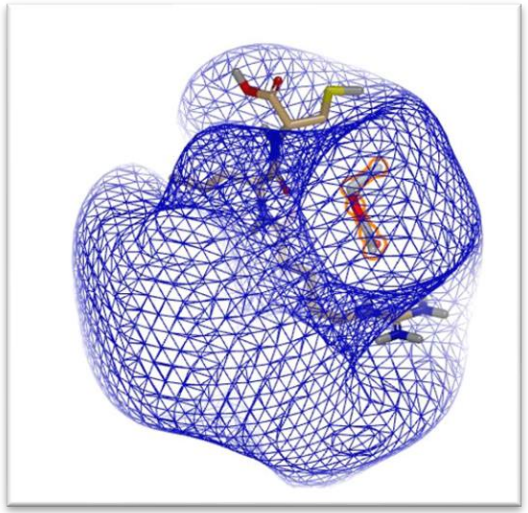

- Docking box generation 10 conformers for each peptide for identification of most probable bond sites and energy quantification involved in the docking simulation
- From 1 to 200 conformers for each volatile compound
- Binding score: average of all conformers

[Mascini, Marcello, et al. "Tailoring gas sensor arrays via the design of short peptides sequences as binding elements." *Biosensors and Bioelectronics* 93 (2017): 161-169.

Hp-DNA

hpDNA has been used as molecular switch for optical and electrochemical sensing

- **The loop can be used as sensing elements also for VOCs**
- **A virtual screening of the entire library sequences of the loops is possible**
- **hpDNA can be easily bound to metal nanoparticles (AuNPs)**

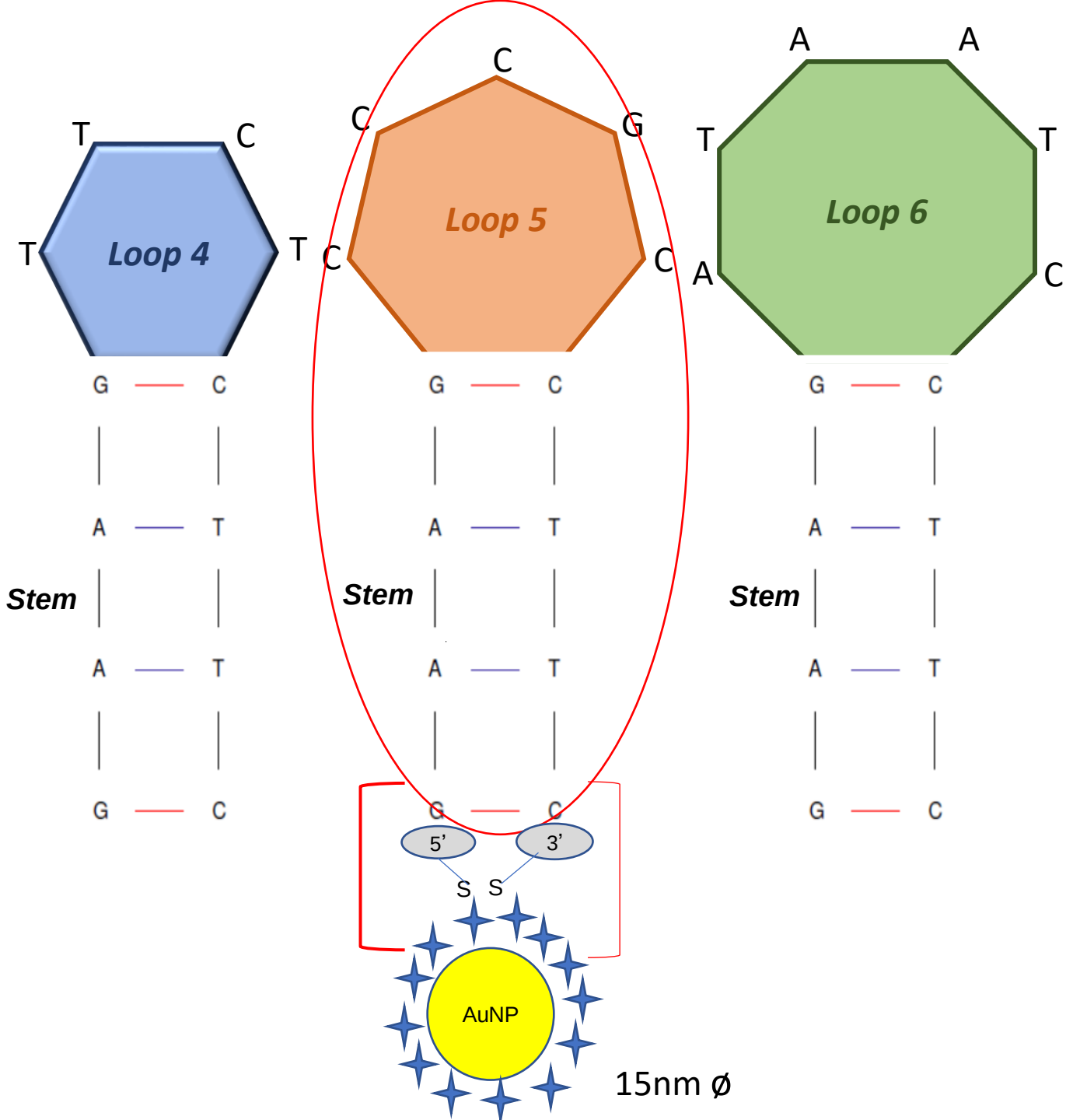

Virtual screening of hp-DNA

Virtual screening procedure was aimed to test the virtual binding affinities of the hairpin loop versus different chemical classes:

- **Alcohols (14 molecules);**
- **Aldehydes (13 molecules);**
- **Esters (18 molecules);**
- **Ketones (5 molecules).**

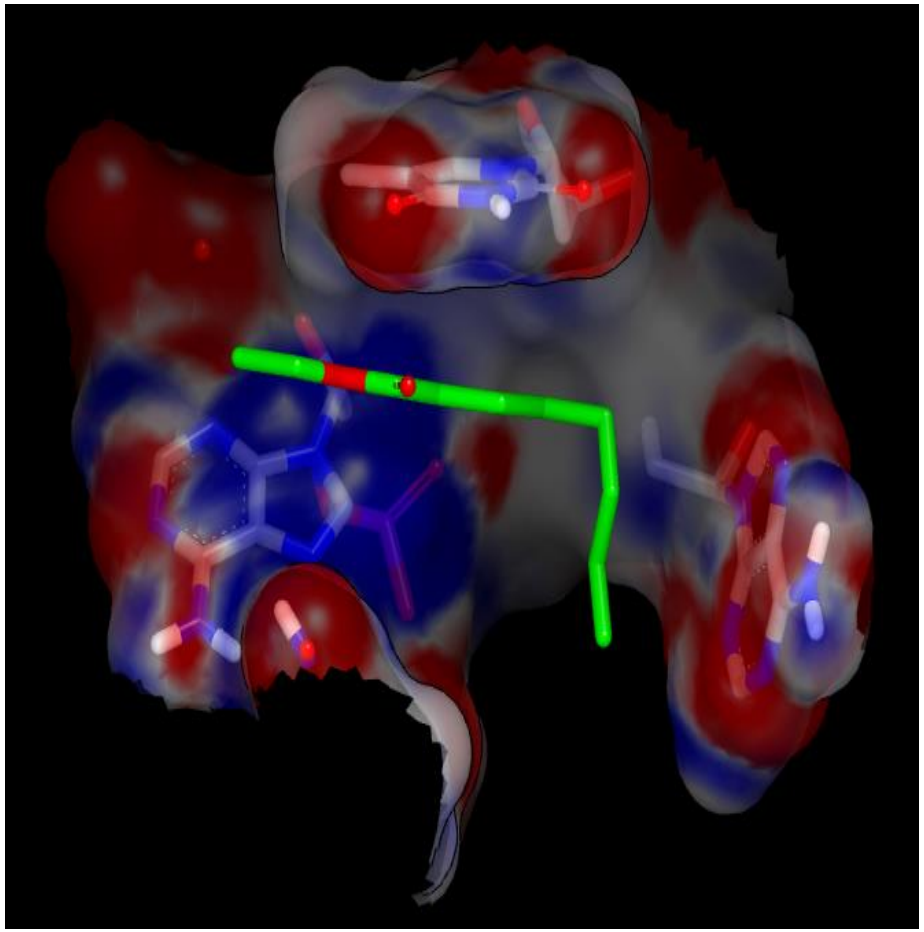

Molecular Modeling : octanal-ATAATC

OEDocking 3.0.0; VIDA version 4.1.1; OMEGA

Electronic nose sequences…

n=20

TGKFC

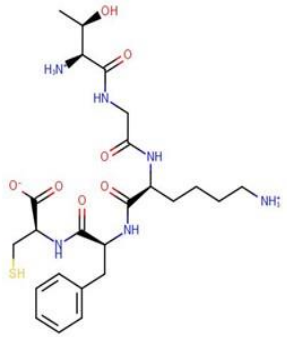

KSDSC

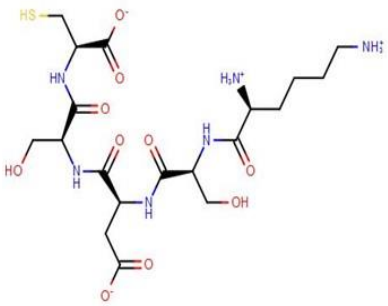

IHRIC

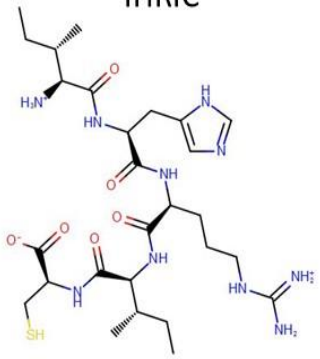

LGFDC

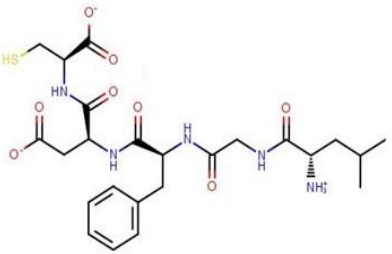

WHVSC

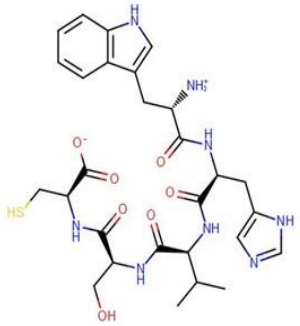

LAWHC

GAAGCGGGCTTC

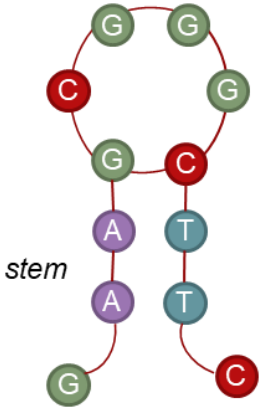

GAAGCCCGACTTC

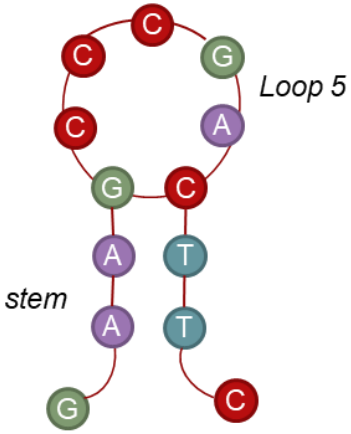

GAAGATAATCCTTC

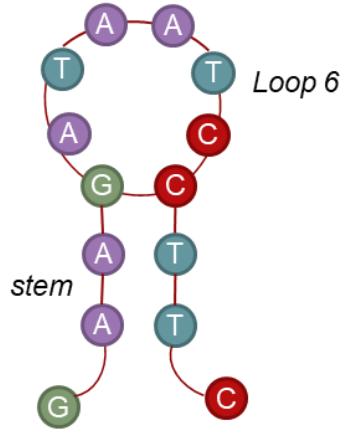

E-nose analysis

UNIVERSITÀ DEGLI STUDI DI TERAMO

1

5 µL of the AuNPs-hpDNA and ZnO-Peptide suspension on each side of the QCM

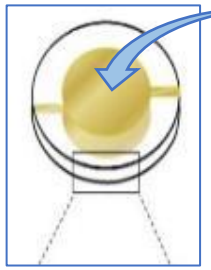

3

✓ **Aroma release in headspace of gas-tight bottle**

5

Measurement of aroma compounds; the frequency shift was taken as analitical signal

4

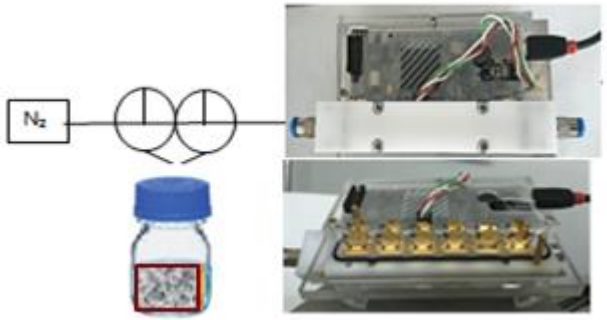

2

✓ **The samples was introduced in a gas-tight bottle (100 mL)**

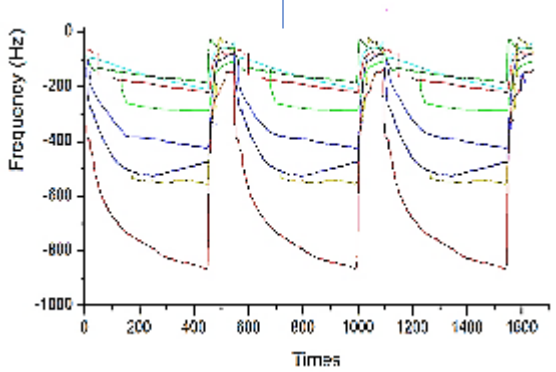

SPME-GC/MS analysis

UNITE UNIVERSITÀ DEGLI STUDI DI TERAMO

headspace analysis

Desorption

Nist library

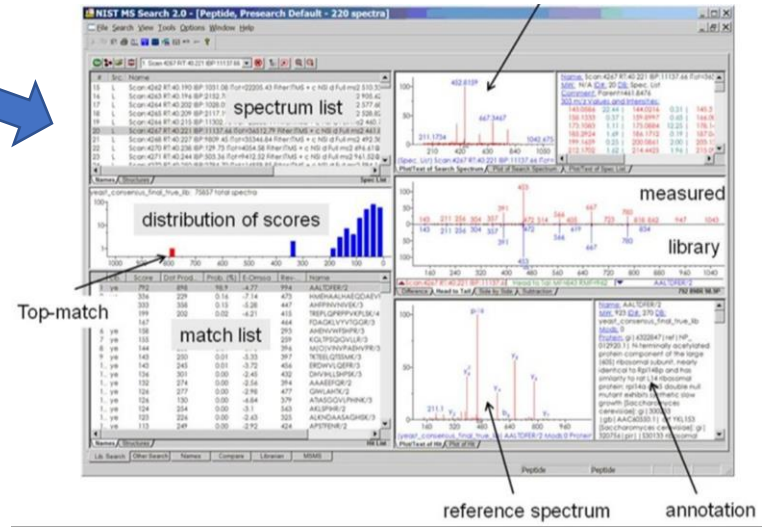

Confirmed by Retention index…

Example…

Peak no.	RT[a] (min)	RI_{lit}[b]	RI_{cal}[c]	Identification[d]	Metabolite	MF[e]	*m/z*[f]	Similarity (%)	Peak area (×10⁶ area units) ± RSD (%)					
									DVB/CAR/PDMS[g]	PDMS[g]	CAR/PDMS[g]	PDMS/DVB[g]	PEG[g]	PA
1	1.42	-	908	MS, RI	Isoprene	C_5H_8	32, 67, 53	96	0.1 ± 7.8	-	0.4 ± 1.2	0.7 ± 1.5	-	-
2	3.92	1007	1016	MS, RI, ST	α-Pinene	$C_{10}H_{16}$	93, 77, 121	93	0.7 ± 9.7	1.0 ± 2.8	0.6 ± 2.9	0.5 ± 2.5	0.1 ± 3.1	0.02 ± 8.2
3	4.77	1075	1057	MS, RI	Camphene	$C_{10}H_{16}$	93, 121, 41	94	0.04 ± 8.7	0.2 ± 9.5	0.1 ± 8.5	0.3 ± 3.2	0.01 ± 5.5	-
4	5.73	1116	1107	MS, RI, ST	β-Pinene	$C_{10}H_{16}$	93, 41, 69	91	2.4 ± 1.2	5.8 ± 3.9	3.0 ± 3.2	3.2 ± 8.0	0.5 ± 2.7	0.1 ± 1.3
5	8.79	1145	1135	MS, RI, ST	β-Myrcene	$C_{10}H_{16}$	93, 69, 41	97	153.3 ± 1.1	191.1 ± 1.7	159.3 ± 1.9	126.7 ± 1.9	27.7 ± 2.5	7.6 ± 5.0
6	9.53	1180	1172	MS, RI, ST	Limonene	$C_{10}H_{16}$	68, 93, 79	93	1.3 ± 1.3	1.1 ± 5.0	1.2 ± 5.0	1.7 ± 7.6	0.3 ± 2.9	0.1 ± 2.1
7	10.01	1185	1182	MS, RI	β-Phellandrene	$C_{10}H_{16}$	93, 77, 136	95	1.1 ± 2.6	0.2 ± 6.8	0.9 ± 5.1	1.1 ± 1.0	-	-
8	11.64	1242	1246	MS, RI	*trans*-β-Ocimene	$C_{10}H_{16}$	93, 79, 41	89	0.1 ± 1.2	0.1 ± 7.4	0.1 ± 1.1	0.1 ± 2.4	0.01 ± 4.2	-
9	11.79	1262	1267	MS, RI, ST	α-Terpinene	$C_{10}H_{16}$	93, 136, 77	91	0.1 ± 1.4	0.1 ± 3.3	0.1 ± 2.6	0.1 ± 2.7	0.01 ± 3.5	-
10	12.48	1274	1279	MS, RI	*cis*-β-Ocimene	$C_{10}H_{16}$	93, 76, 41	92	2.1 ± 1.3	2.6 ± 3.2	2.2 ± 2.5	1.5 ± 2.5	0.2 ± 1.0	0.03 ± 1.3
11	13.15	-	1290	MS, RI, ST	o-Cymene	$C_{10}H_{14}$	119, 32, 134	95	0.1 ± 1.9	0.1 ± 2.7	0.1 ± 1.3	0.04 ± 1.3	0.01 ± 1.2	-
12	13.75	1284	1280	MS, RI	α-Terpinolene	$C_{10}H_{16}$	93, 121, 136	97	0.1 ± 3.4	0.1 ± 3.6	0.1 ± 1.0	0.1 ± 2.8	0.01 ± 1.1	-
13	22.88	1295	1305	MS, RI	Perillene	$C_{10}H_{14}O$	69, 81, 150	96	0.2 ± 1.5	0.2 ± 8.6	0.2 ± 2.9	0.2 ± 2.5	0.03 ± 2.3	-
14	26.07	1476	1481	MS, RI	Ylangene	$C_{15}H_{24}$	105, 119, 161	95	0.4 ± 2.0	0.2 ± 5.8	0.3 ± 2.0	0.2 ± 3.2	-	-
15	26,64	1480	1491	MS, RI	α-Cubebene	$C_{15}H_{24}$	161, 119, 105	91	1.2 ± 2.0	0.8 ± 1.7	0.8 ± 1.6	0.7 ± 3.5	0.1 ± 2.2	0.3 ± 1.6
16	33.62	1663	1621	MS, RI, ST	α-Humulene	$C_{15}H_{24}$	133, 93, 69	96	48.1 ± 7.5	52.8 ± 2.0	41.4 ± 1.5	36.8 ± 3.7	10.9 ± 2.6	3.1 ± 8.0
17	38.63	1657	1665	MS, RI, ST	β-Caryophyllene	$C_{15}H_{24}$	93, 80, 121	93	42.4 ± 4.1	21.3 ± 2.3	16.8 ± 1.9	15.4 ± 3.6	3.6 ± 2.5	1.0 ± 2.2
18	39.90	1681	1687	MS, RI	γ-Muurolene	$C_{15}H_{24}$	161, 105, 119	88	1.7 ± 2.7	1.3 ± 2.8	0.9 ± 1.8	0.8 ± 1.4	0.6 ± 3.3	0.1 ± 1.9
19	41.40	1566	1554	MS, RI	Methyl geranate	$C_{11}H_{18}O_2$	69, 41, 114	90	3.7 ± 1.1	3.1 ± 4.2	1.3 ± 3.1	2.3 ± 2.0	0.4 ± 2.8	0.1 ± 3.2
20	41.89	1724	1713	MS, RI, ST	α-Selinene	$C_{15}H_{24}$	189, 161, 93	92	0.8 ± 9.8	0.2 ± 2.3	0.2 ± 6.8	0.4 ± 4.1	0.2 ± 3.0	0.04 ± 2.3
21	42.50	-	1744	MS, RI	α-Muurolene	$C_{15}H_{24}$	105, 161, 93	89	0.3 ± 2.5	0.3 ± 1.8	0.2 ± 1.6	0.2 ± 4.1	0.1 ± 3.6	0.02 ± 1.4
22	44.59	1749	1740	MS, RI, ST	(+)-δ-Cadinene	$C_{15}H_{24}$	161, 134, 119	89	1.9 ± 2.2	1.6 ± 1.8	1.0 ± 1.5	1.0 ± 4.2	0.4 ± 2.6	0.1 ± 1.0
23	45.88	-	1755	MS, RI, ST	Cubenene	$C_{15}H_{24}$	119, 105, 161	93	0.3 ± 5.4	0.2 ± 5.7	0.1 ± 1.2	0.2 ± 4.4	0.1 ± 3.8	0.01 ± 7.1
24	46.60	-	1769	MS, RI	Naphthalene H4,7DM 1R[h]	$C_{15}H_{24}$	105, 161, 91	96	0.2 ± 2.5	0.1 ± 2.1	0.1 ± 2.0	0.1 ± 4.7	0.1 ± 6.3	0.01 ± 9.8
25	48.27	-	1780	MS, RI	β-Fenchene	$C_{10}H_{16}$	79, 32, 67	95	0.1 ± 3.0	0.1 ± 4.6	0.02 ± 2.7	0.04 ± 5.2	0.01 ± 1.1	0.01 ± 1.0
26	49.30	1800	1789	MS, RI, ST	3-Carene	$C_{10}H_{16}$	69, 93, 41	98	0.9 ± 2.5	0.4 ± 1.1	0.3 ± 2.3	0.4 ± 5.0	0.3 ± 1.2	0.04 ± 8.0
27	51.68	1825	1835	MS, RI, ST	*cis*-Geraniol	$C_{10}H_{18}O$	69, 41, 93	92	0.2 ± 2.0	0.1 ± 3.9	0.1 ± 3.2	0.1 ± 2.0	0.1 ± 1.0	-
					Total peak area (×10⁶)				**263.7**	**285.0**	**231.8**	**194.4**	**45.6**	**12.4**
					Average RSD (%)				**3.4**	**3.9**	**2.7**	**3.4**	**2.8**	**3.9**
					No. metabolite by fiber				**27**	**26**	**27**	**27**	**24**	**17**

a) Retention time (min).
b) Kovat's retention index reported in the literature for BP-20 capillary column or equivalents [53].
c) Kovat's retention index relative n-alkanes(C_8–C_{20}) on a BP-20 capillary column.

[4] Gallily, R., Yekhtin, Z. and Hanuš, L.O., 2018. The Anti-Inflammatory Properties of Terpenoids from Cannabis. Cannabis and cannabinoid research, 3(1), pp.282-290.

Headspace Volatile Evaluation of Carrot Samples Comparison of GC/MS and AuNPs-hpDNA-Based E-Nose

UNITE UNIVERSITA DEGLI STUDI DI TERAMO

- Monitoring and control of vegetable ripening are important parameters in the food industry, since the maturation state during harvest, storage and distribution on the market defines the quality of the finished product;
- To prevent enzymatic reactions during processing, storage and thawing, the packaged carrots were blanched at 95 °C for 8 min in a water bath
- 3 g of blanched carrots were placed in 20 ml gas-tight vials and hermetically sealed with a gas-tight septum. A total of 24 vials were prepared for each temperature tested (-18 °C, 4 °C, 25 °C, 40 °C), in order to have three replicates (three different vials) for each day of measurement (1, 4, 8, 12, 19, 26 days). Thus, a total of 140 vials for E-nose and GC-MS have been analyzed. Each vial was used only once for either the GC-MS or E-nose measurement and the relative sample was discarded.

SPME-GC/MS

UNITE UNIVERSITÀ DEGLI STUDI DI TERAMO

	GC area (%)																			
	Storage time (days)																			
	-18 °C					4°C						25 °C						40 °C		
Volatile compounds	1	4	8	12	19	1	4	8	12	19	26	1	4	8	12	19	26	1	4	8	12
α-phellandrene	n.d	n.d	n.d	n.d	n.d	1	1	1	1	1	n.d	n.d**	1	n.d	n.d	1	n.d	7	1	n.d	n.d
β-phellandrene	2	1	2	1	1	3	3	2	1	4	1	n.d	3	1	1	2	n.d	n.d	n.d	n.d	n.d
terpinolene	n.d	n.d	1	1	0	1	1	1	n.d	1	n.d	n.d	1	n.d	n.d	1	n.d	n.d	n.d	n.d	n.d
α-pinene	14	9	12	12	10	14	12	14	14	18	8	12	7	12	11	15	2	n.d	10	15	5
(-) -β-pinene	3	2	3	3	3	3	3	3	3	3	2	2	3	2	2	3	1	n.d	n.d	n.d	2
β-pinene	3	2	3	2	6	5	6	3	3	5	1	2	6	1	1	4	n.d	5	3	3	2
Octanal	1	1	n.d	n.d	n.d	1	1	1	1	n.d	n.d	1	n.d	n.d	n.d	n.d	n.d	n.d	n.d	n.d	n.d
γ-terpinene	7	8	9	10	7	8	9	7	8	4	1	12	7	6	5	7	n.d	21	9	9	5
β-farnesene	1	1	1	1	1	1	1	1	1	n.d	1	1	1	1	1	1	2	n.d	n.d	n.d	n.d
α-caryophyllene	1	1	1	1	2	2	1	1	1	1	5	1	2	1	2	1	2	n.d	n.d	n.d	n.d
β-copaene	2	2	2	n.d	4	2	2	3	n.d	n.d	n.d	2	1	2	2	2	5	n.d	n.d	n.d	n.d
myristicin	1	1	1	1	2	1	1	1	1	1	5	2	1	2	n.d	1	4	n.d	n.d	n.d	n.d
elemicin	n.d	1	n.d	n.d	n.d	n.d	n.d	1	n.d	n.d	4	1	n.d	1	1	n.d	2	n.d	n.d	n.d	n.d
butane-2,3-diol	n.d	n.d	n.d	n.d	n.d	n.d	n.d	n.d	n.d	n.d	n.d	n.d	n.d	2	2	5	13	n.d	n.d	n.d	3
acetoin	n.d	n.d	n.d	n.d	n.d	n.d	n.d	n.d	n.d	n.d	n.d	n.d	n.d	9	3	6	15	5	3	5	6
ethanol	n.d	n.d	n.d	n.d	n.d	n.d	n.d	n.d	n.d	n.d	n.d	n.d	n.d	n.d	n.d	n.d	n.d	5	n.d	n.d	6
lactamide	n.d	n.d	n.d	n.d	n.d	n.d	n.d	n.d	n.d	n.d	n.d	n.d	n.d	n.d	n.d	n.d	n.d	4	11	16	7
3-methylbutan-1-ol	n.d	n.d	n.d	n.d	n.d	n.d	n.d	n.d	n.d	n.d	n.d	n.d	n.d	n.d	n.d	1	2	1	3	3	3

*(mean value of n=3 repetitions); **n.d.: not detected.

Results of the gas-chromatographic (GC) analysis of the headspace of carrots samples. Data are expressed as % of the total GC area*.

E-NOSE

UNIVERSITÀ DEGLI STUDI DI TERAMO

Carrots Sample	CGGG	TTGG	CTGCAA	CAGC	TAAGT	AAGTA	ATAATC	CCCGA
25°C/1	145	199	314	187	409	566	686	147
4°C/1	118	221	132	155	417	468	564	107
-18°C/1	111	241	199	150	415	485	529	127
25°C/4	103	259	323	164	495	575	645	146
4°C/4	107	230	317	159	535	492	608	156
-18°C/4	101	208	244	155	577	513	603	165
25°C/8	148	228	339	237	544	462	787	216
4°C/8	130	204	179	174	480	632	701	180
-18°C/8	129	188	197	140	498	493	603	175
25°C/12	127	201	311	182	529	564	716	192
4°C/12	126	180	414	147	470	553	660	141
-18°C/12	105	205	403	166	602	495	664	148
25°C/19	87	131	120	100	374	515	565	135
4°C/19	86	257	301	145	483	696	600	160
-18°C/19	114	224	307	118	421	662	607	150
25°C/26	46	88	289	161	146	583	494	140
4°C/26	64	118	370	101	358	497	576	145
40°C/1	41	98	250	176	169	468	755	175
40°C/3	51	146	252	192	160	507	733	214
40°C/4	53	143	235	194	168	507	693	167
40°C/9	45	217	263	150	239	453	686	168

Frequency shift (Hz) response of the HpDNA sensors array for the carrots samples. The coefficient of variation calculated using three measurements taken in three different days was in all cases below 15%.

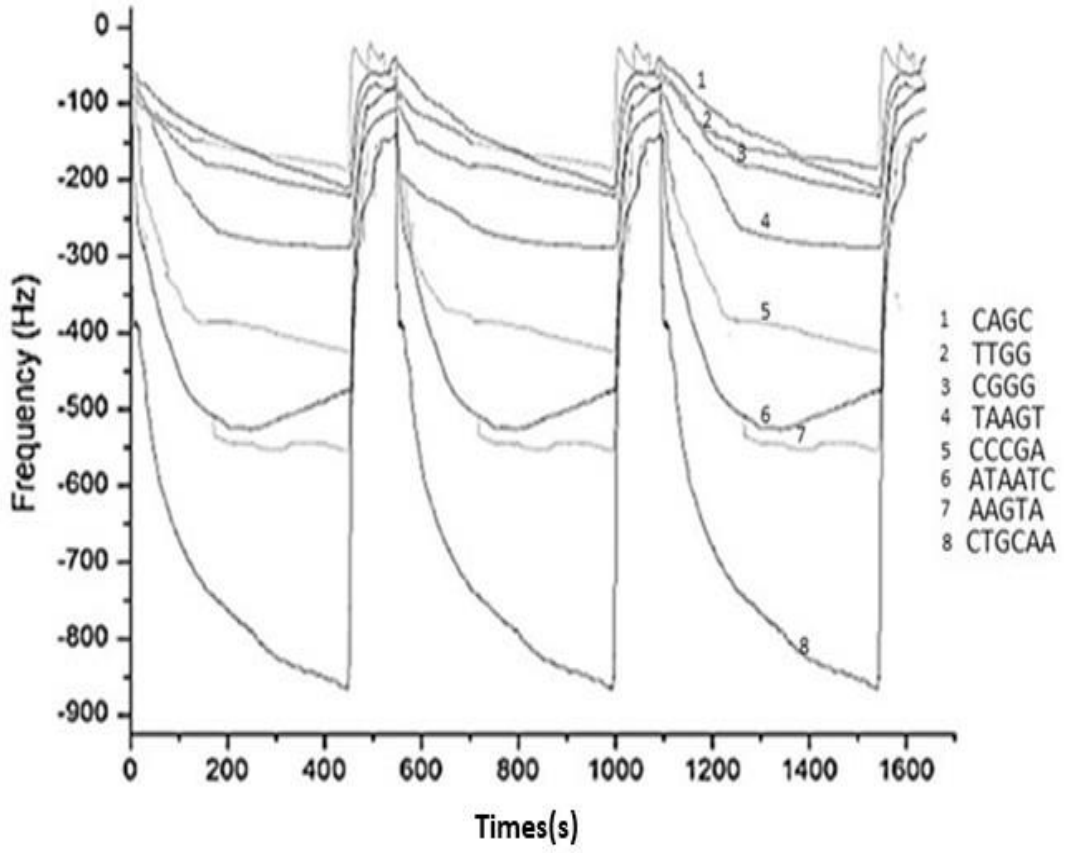

Frequency signal recorded with AuNPs-hpDNA testing carrots samples in triplicate

GC-MS

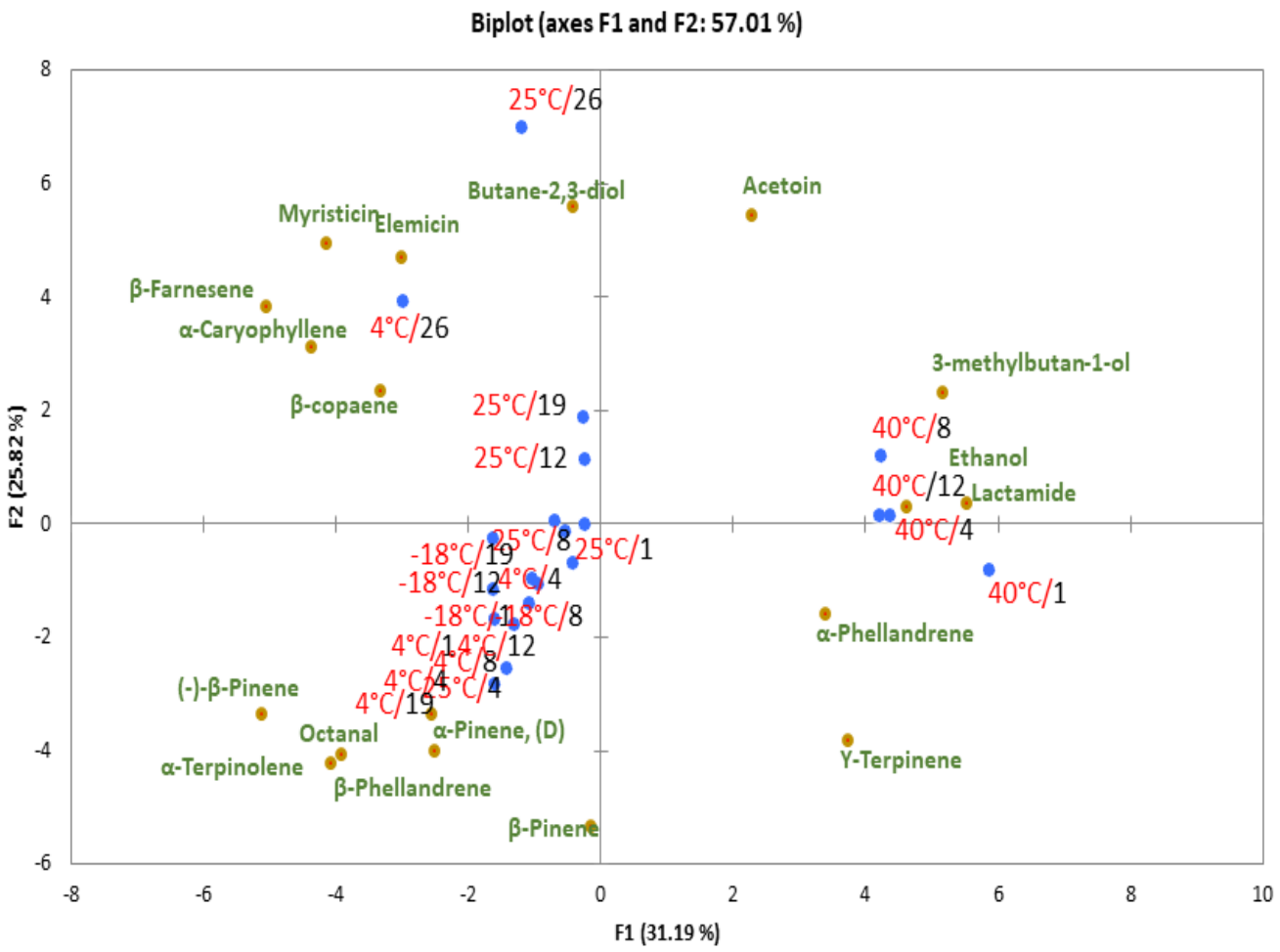

PCA of the GC-MS/SPME response of carrot samples stored for different time at various temperature. Data are expressed in (Relative Abundance %) before PCA

E-nose

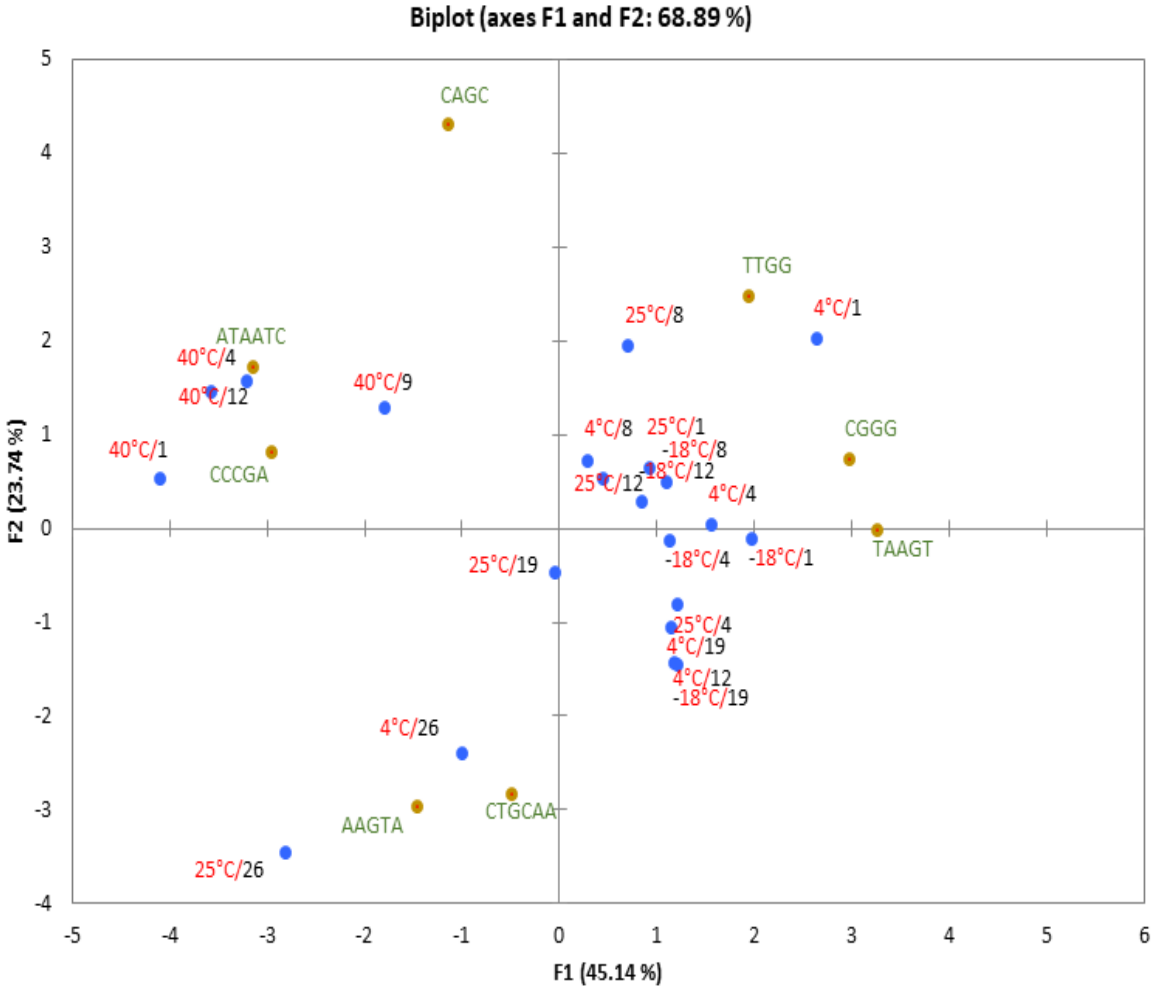

PCA biplot (scores and loadings) of the E-nose response to carrots samples. Data were normalized before PCA

Surface plasmon resonance imaging

home-made SPRI system

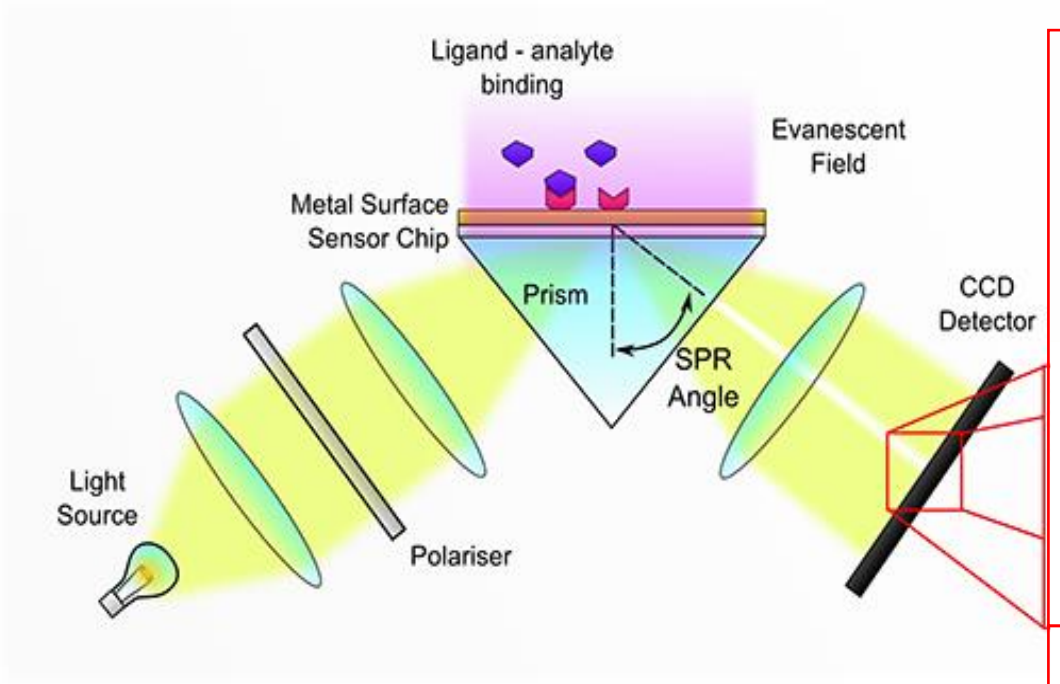

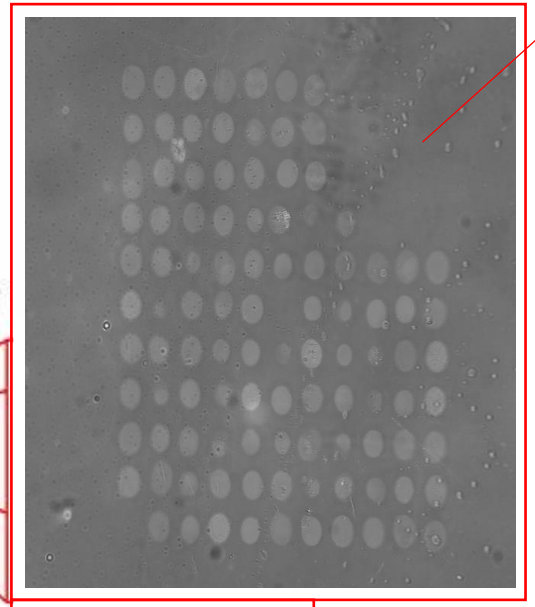

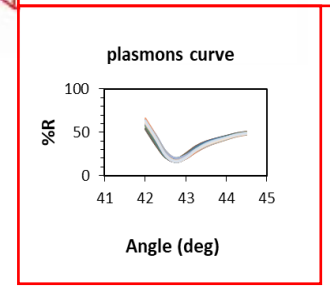

- *104 spot*
- *12 peptides at different concentration: 200µM and 400µM*
- *14 hpDNA: 16.8µM*
- *1.2 nL volume drop (≤1mm)*

a)

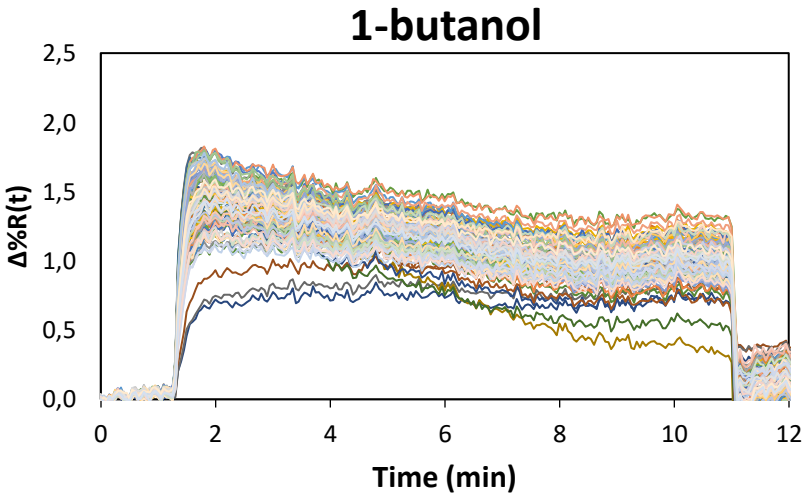

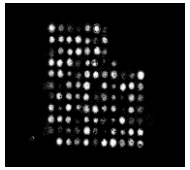

1-butanol

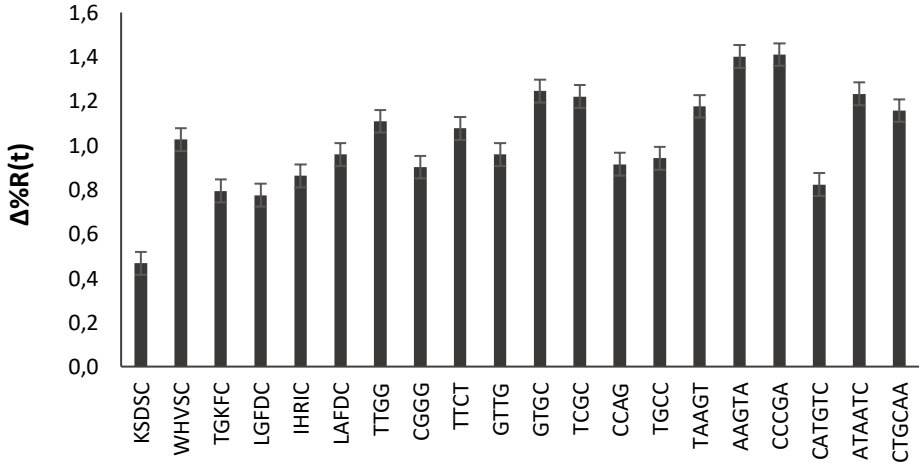

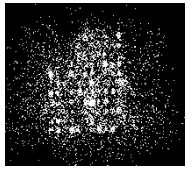

1-pentanol

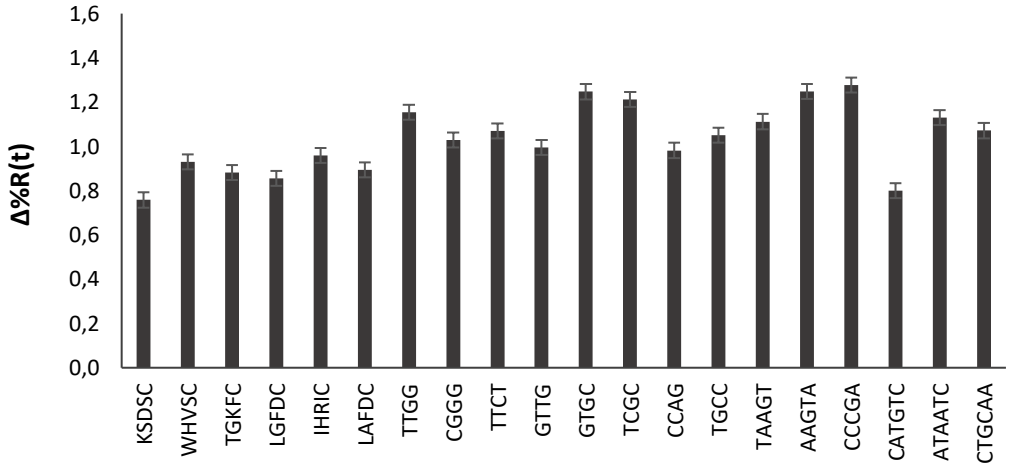

b)

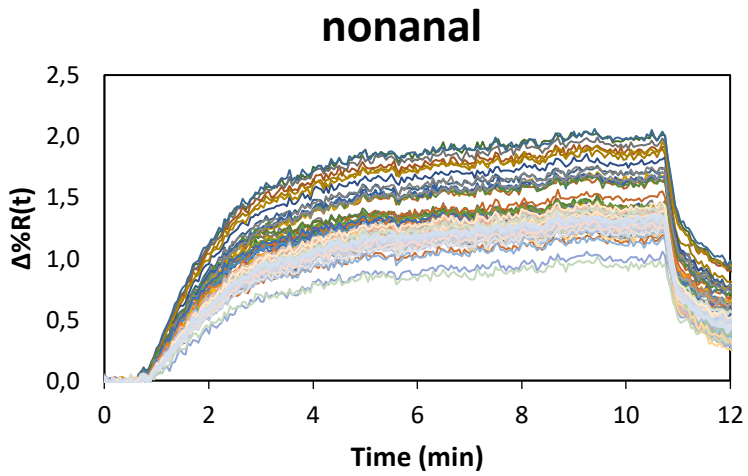

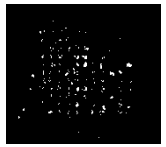

hexanal

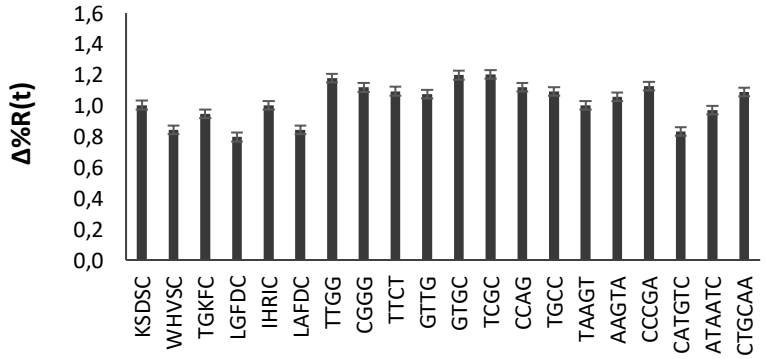

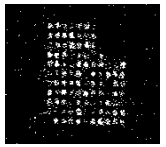

nonanal

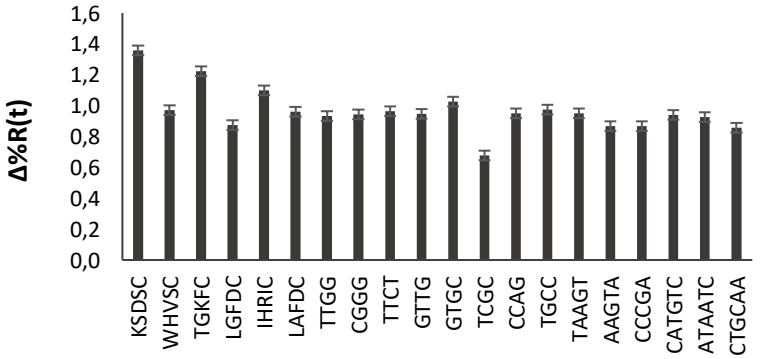

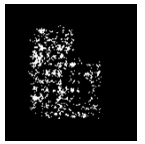

trans-2-nonenal

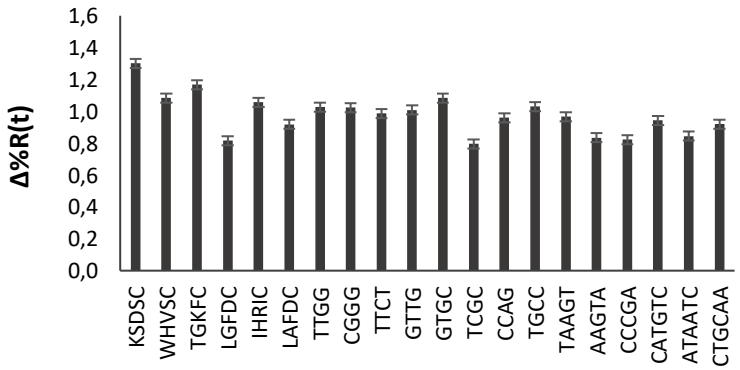

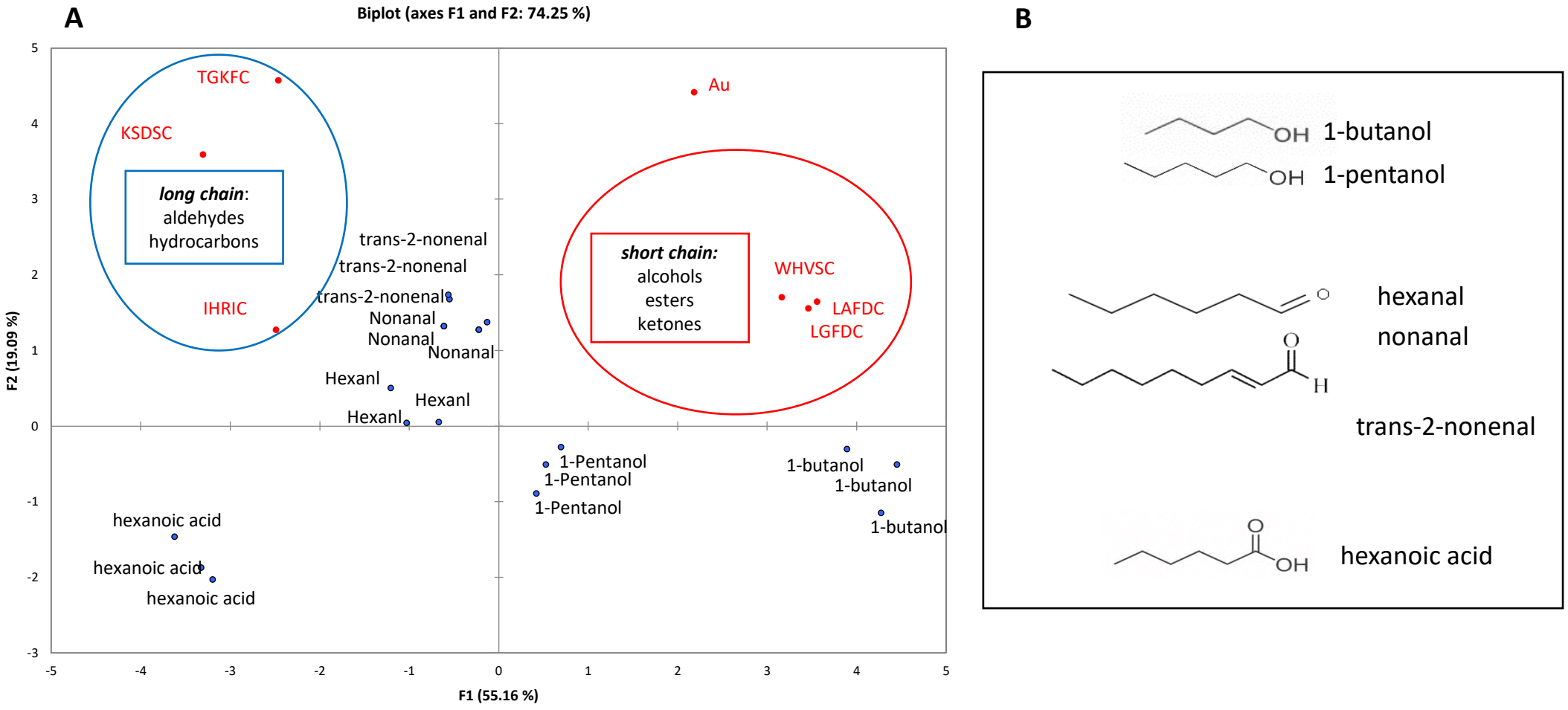

(A) PCA (*loading* and *score* plots) for the discrimination of different VOCs with different penta-peptides; **(B)** Explain the different chemical structures of VOCs tested: 1-butanol, 1-pentanol, hexanal, trans-2-nonenal, hexanoic acid

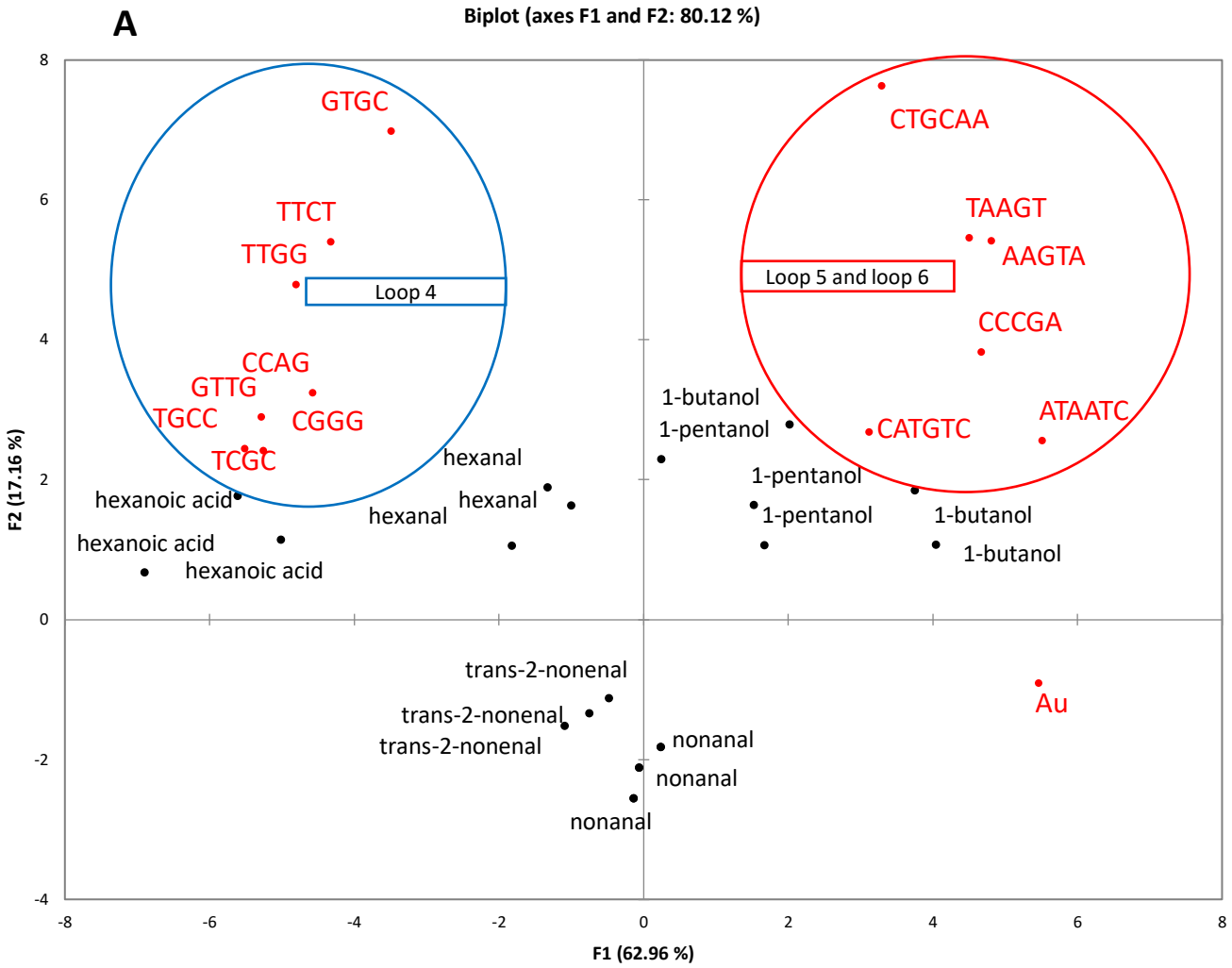

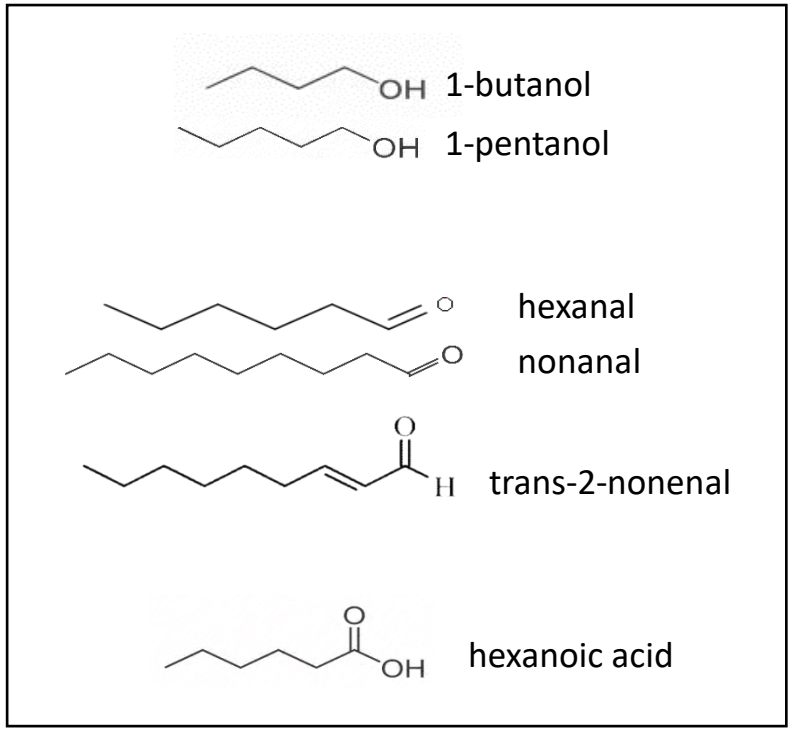

(A) PCA (*loading* and *score* plots) for the discrimination of different VOCs with different hpDNA; **(B)** Explain the different chemical structures of VOCs tested: 1-butanol, 1-pentanol, hexanal, trans-2-nonenal, hexanoic acid

Agglomerative hierarchical Clustering (AHC) analysis with peptide and hpDNA

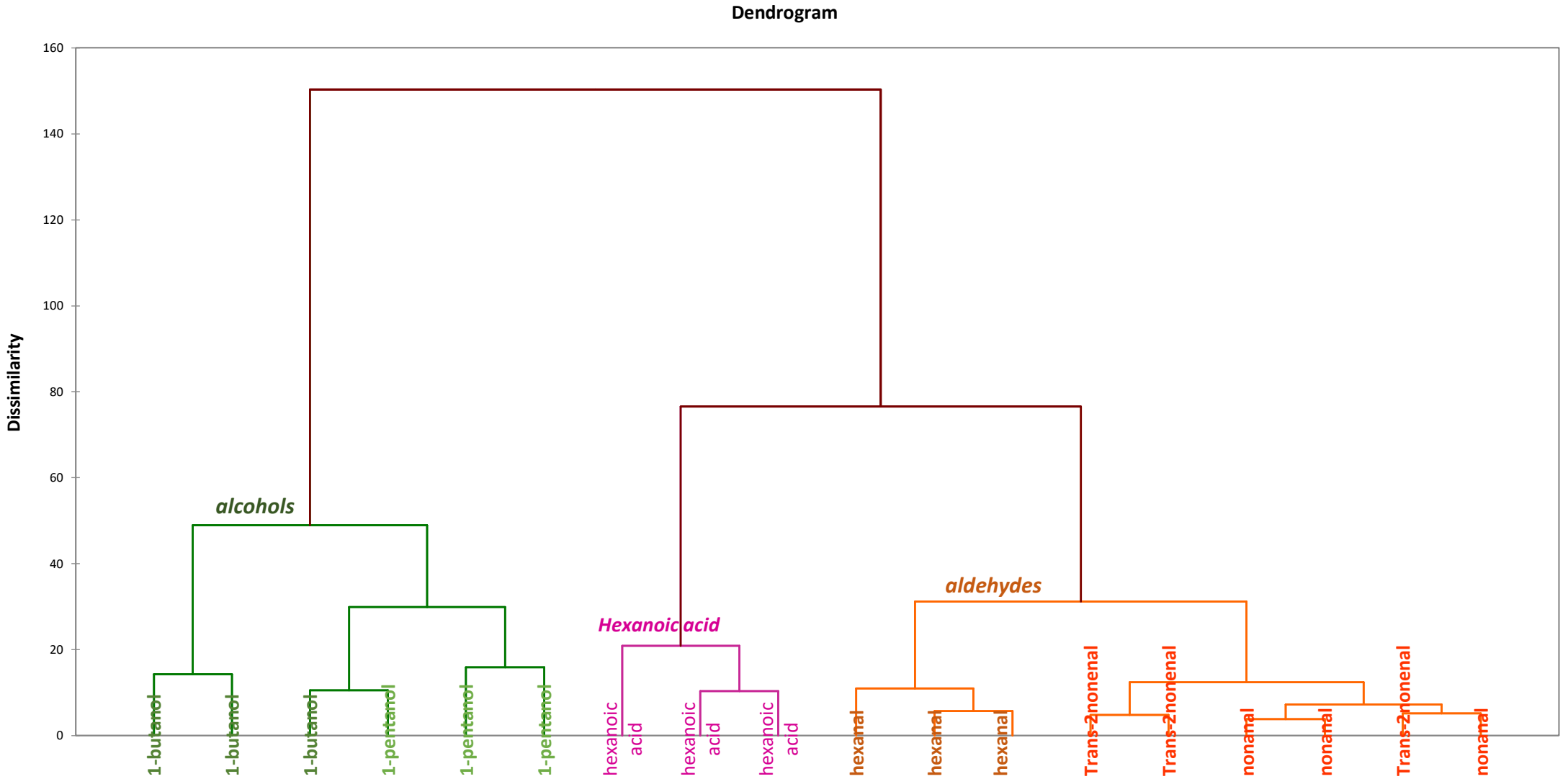

sensors

MDPI

Article

A Study of Diagnostic Accuracy Using a Chemical Sensor Array and a Machine Learning Technique to Detect Lung Cancer

Chi-Hsiang Huang [1,2], Chian Zeng [3], Yi-Chia Wang [1,2], Hsin-Yi Peng [3], Chia-Sheng Lin [4], Che-Jui Chang [3,5] and Hsiao-Yu Yang [3,6,*]

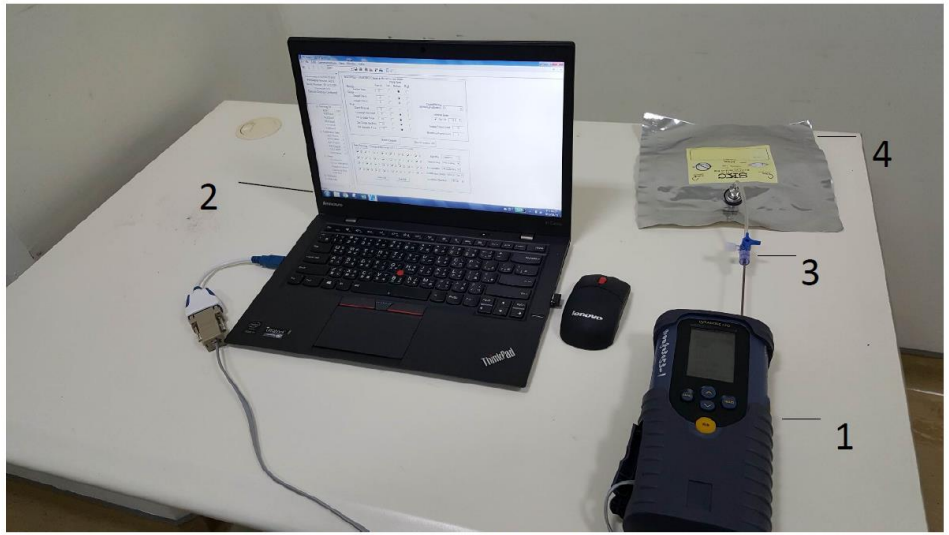

Figure S1. Experimental setup for the analysis of alveolar air consisting of a (1) E-nose, (2) computer, (3) three-way valve and (4) Tedlar bag.

Legend: The bags were connected with the necessary fixture, including an airtight PVC tube and a three-way valve for connection to the E-nose.

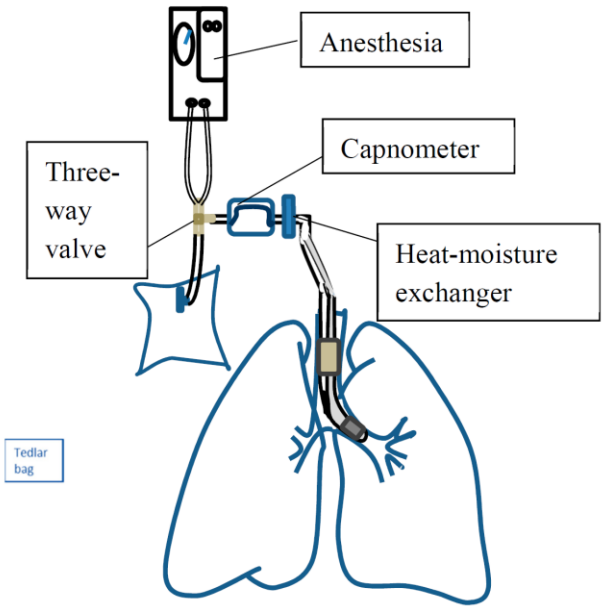

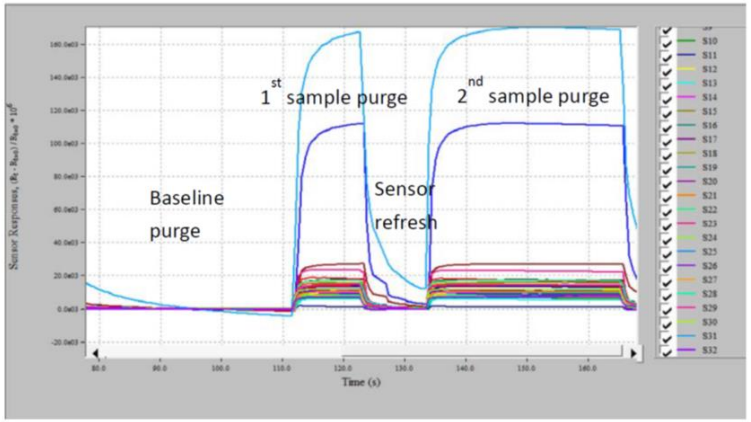

Figure S2. Desired waveforms for Cyranose320.

Legend: The setting comprised 10 seconds of a baseline purge and 40 seconds of a sample purge, which was sufficient for most sensors to reach the steady-state, followed by 10 seconds of a wash-out to return to the baseline.

Early detection of lung cancer with good specificity

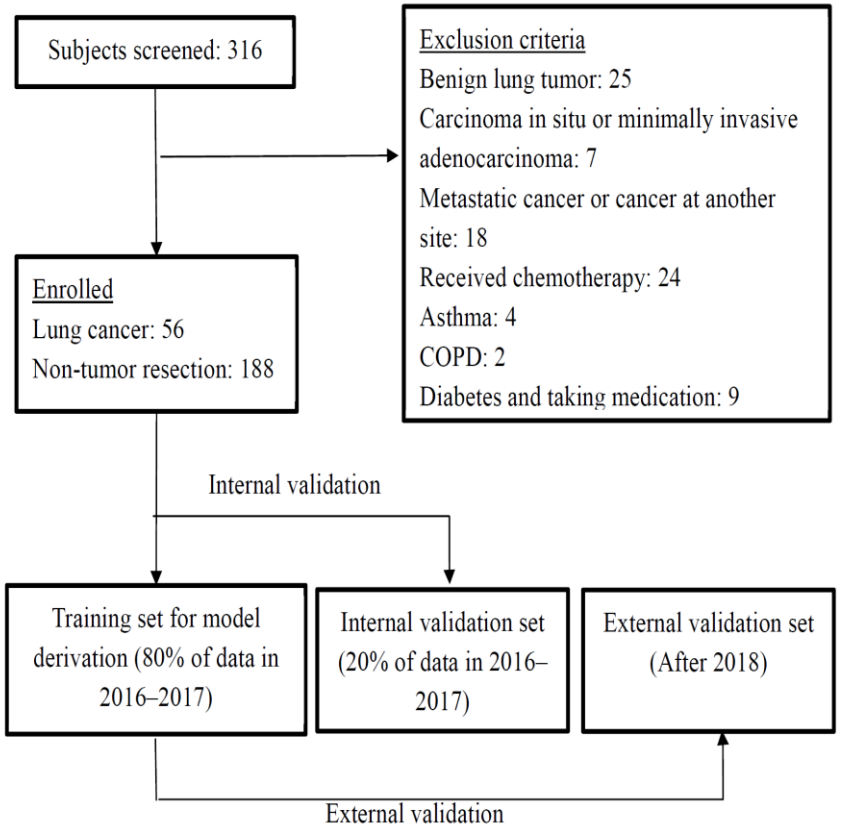

Figure 2. Flow diagram depicting the inclusion and exclusion of the study subjects. We employed an independent external validation set and conducted a repeated double cross-validation. The repeated double cross-validation used two nested loops. The inner loop used the study subjects enrolled between 2016 and 2017 as a calibration set for model selection and parameter optimization and were divided into a training set (80%) and an internal validation set (20%). The outer loop used the prediction model established from the calibration set to externally validate the study subjects enrolled in 2018.

Model	Sensitivity	Specificity	PPV	NPV	FP	FN	Accuracy
LDA internal validation	100.0%	88.6%	60.0%	100.0%	12.4%	0.0%	90.2%
LDA external validation	75.0%	96.6%	90.0%	90.3%	3.4%	25.0%	85.4%
SVM internal validation	92.3%	92.9%	85.7%	96.3%	7.1%	7.7%	92.7%
SVM external validation	83.3%	86.2%	71.4%	92.6%	13.8%	16.7%	85.4%

LDA, linear discriminant analysis; SVM, support vector machine; PPV, positive prediction rate; NPV, negative prediction value; FP, false-positive; FN, false-negative.

ANTICANCER RESEARCH *38*: 833-837 (2018)
doi:10.21873/anticanres.12291

Non-invasive Detection of Bladder Tumors Through Volatile Organic Compounds: A Pilot Study with an Electronic Nose

HENDRIK HEERS[1], JOSEF MAXIMILIAN GUT[1], AXEL HEGELE[1], RAINER HOFMANN[1], TOBIAS BOESELT[2], AKIRA HATTESOHL[2] and ANDREAS REMBERT KOCZULLA[2]

[1]*Department of Urology and Paediatric Urology, Philipps-Universität Marburg, Marburg, Germany;*
[2]*Department of Pulmonology, Philipps-Universität Marburg, Marburg, Germany*

Urine samples, standard protocol for bladder tumour diagnosis, cystoscopy

Table I. *Patient demographics.*

	Tumor	Control
Number of individuals	30	30
Mean age [years]	71.3	56.4
Age range [years]	49-86	21-85
Gender (male:female)	24:6	21:9
Smokers	6	6
Former smokers	8	1
Microscopic haematuria	17	7

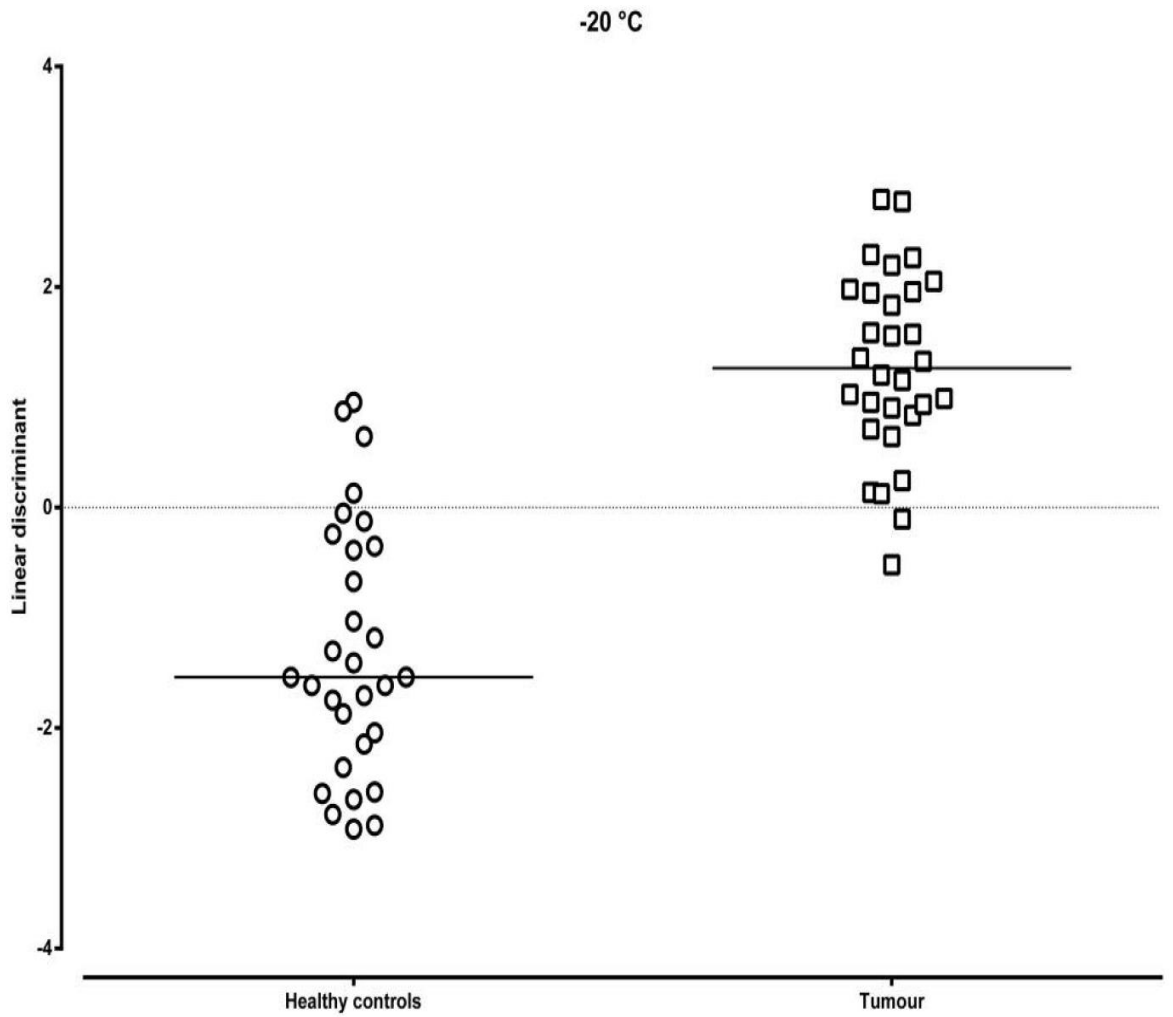

Figure 1. *LDA for samples stored at –20°C.*

Received: 11 June 2019 | First decision: 3 July 2019 | Accepted: 4 December 2019

DOI: 10.1111/apt.15622

Volatile organic compounds in breath can serve as a non-invasive diagnostic biomarker for the detection of advanced adenomas and colorectal cancer

Kelly E. van Keulen[1] | Maud E. Jansen[2,3] | Ruud W. M. Schrauwen[4] | Jeroen J. Kolkman[2,3] | Peter D. Siersema[1]

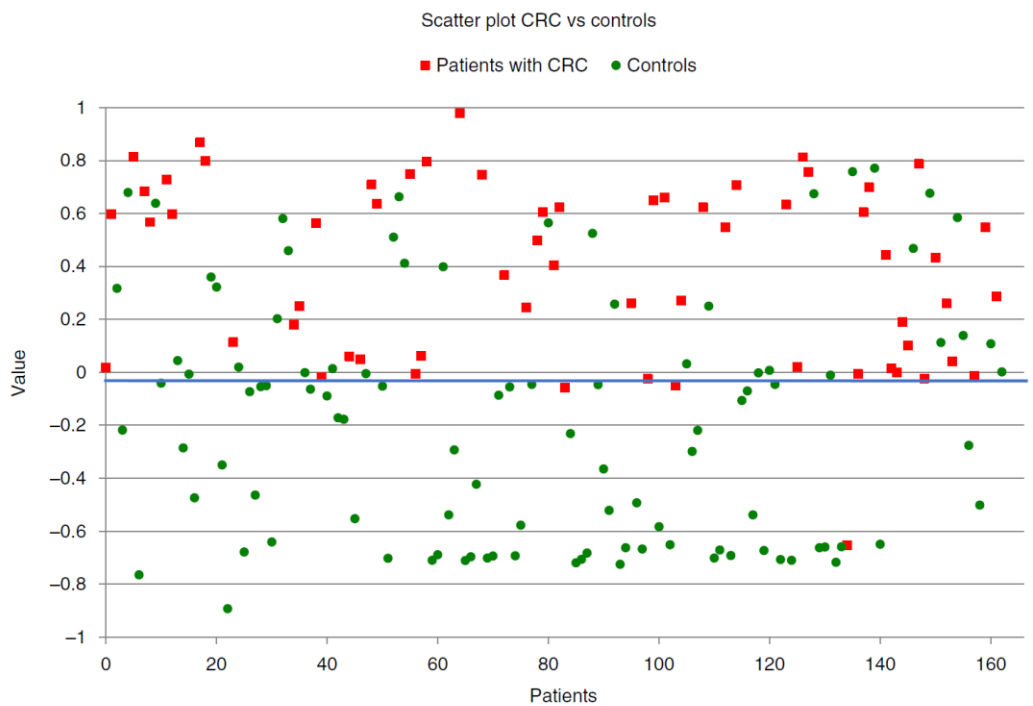

FIGURE 1 Electronic nose used in the study; the Aeonose (The eNose Company). Patients inhale through a carbon filter to prevent the entry of nonfiltered environmental air and breathe into the device through a disposable mouthpiece while wearing a nose clip

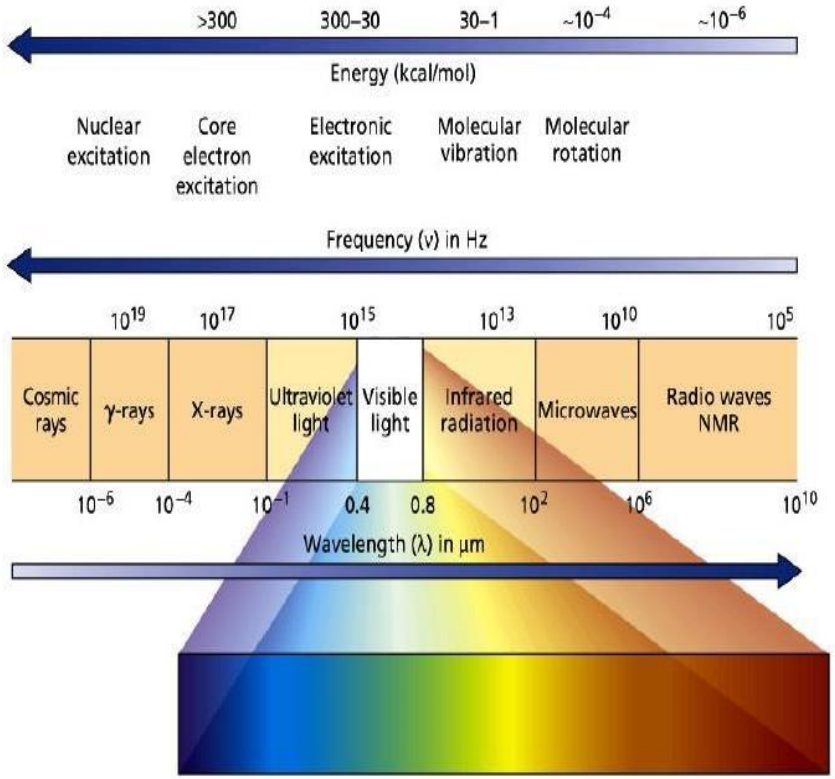

INTRODUCTION OF IR SPECTROSCOPY

- Infrared spectroscopy is an important analytical technique for determining the structure of both inorganic & organic compounds. It is also known as vibrational spectroscopy
- IR radiations lies in the wavelength range of 0.7 - 400 μm.
- IR spectroscopy is based upon selective absorption of IR radiations by the molecule which induces vibration of the molecules of the compound.
- IR instruments are of 2 types namely, dispersive instruments (spectrophotometers) and Fourier transform IR instrument.
- The radiation sources used are incandescent lamp, Nernst glower etc., and the detectors used are thermal and photon detectors.

NATURE OF IR SPECTRA

- IR spectrum is a graph of band intensities on ordinate versus position of band on abscissa.
- Band intensities can be given in terms of transmittance(T) or absorbance(A).
- Position of band can be expressed in terms of wave number (n) or wavelength(λ).
- In IR spectra, wave numbers (n) are used instead of wavelength (λ) for mentioning the characteristic peak as this unit has advantage of being linear with energy of radiation (E) .

$$E = h\,c/\lambda \quad \text{or,} \quad E = h\,c\,n$$

[$n = 1/\lambda$, c= velocity of light, h= Planck's constant]

PRINCIPLE OF IR SPECTROSCOPY

- When the energy in the form of IR is applied and if the applied IR frequency = Natural frequency of vibration, the absorption of IR takes place and a peak is observed.
- Molecules are excited to the higher energy state from the ground state when they absorb IR radiation.
- When a compound is exposed to IR radiation, it selectively absorbs the radiations resulting in vibration of the molecules of the compound, giving rise to closely packed absorption bands, called as IR absorption spectrum.
- The bands correspond to the characteristic functional groups and the bonds present in a chemical substance. Thus, an IR spectrum of a compound is considered as the fingerprint for its chemical identification.

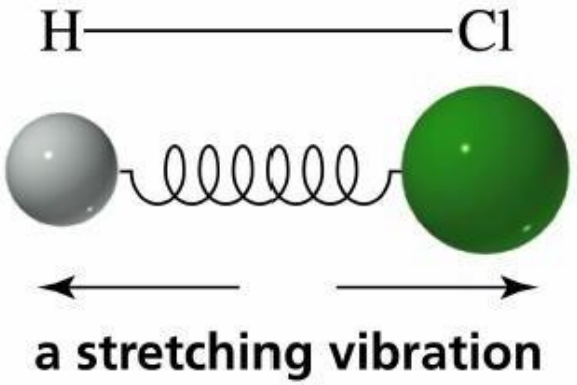

CHANGE IN DIPOLAR MOMENT OF THE MOLECULES MUST OCCUR!

H—Cl

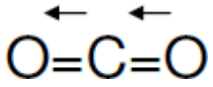

ACTIVE IR STRECHTING

H—H

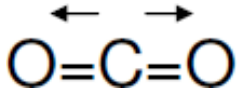

INACTIVE IR STRECHTING

CRITERIA FOR A COMPOUND TO ABSORB IR RADIATION

1. Correct wave length of incident radiation

- A molecules absorbs radiation only when the frequency of the incident radiation is equivalent to the natural frequency of vibration of the part of the molecule.
- After absorption of the correct wave length of radiations, the molecule vibrates at increased amplitude due to absorbed IR energy.
- Example: HCl has natural vibrational frequency of 8.7×10^{13}/s (2890 cm-1). When HCl sample is exposed to IR radiations, only the radiations of frequency 8.7×10^{13}/s are absorbed and remaining are transmitted.

PEAK POSITION

$$\tilde{\nu} = \frac{1}{2\pi c}\sqrt{\frac{k}{m^*}}$$

k = bond strenght

$m^* = m_A\, m_B / (m_A + m_B)$

O–H > N–H > C–H

BOND STRENGHT

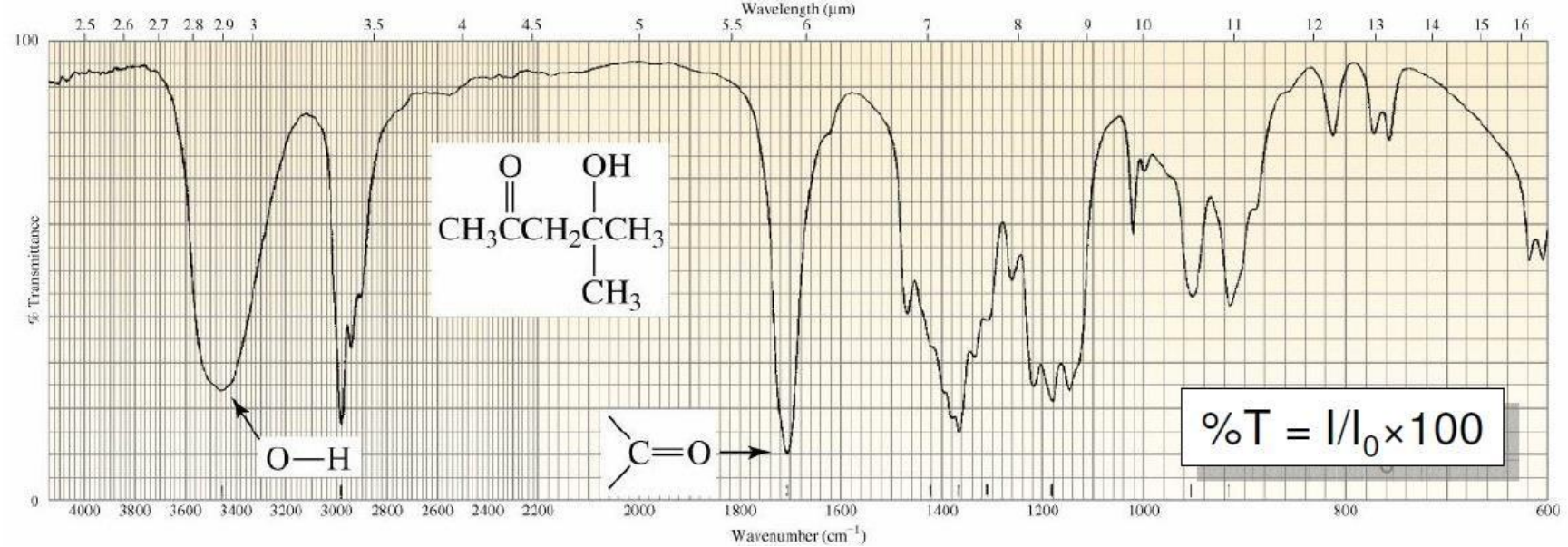

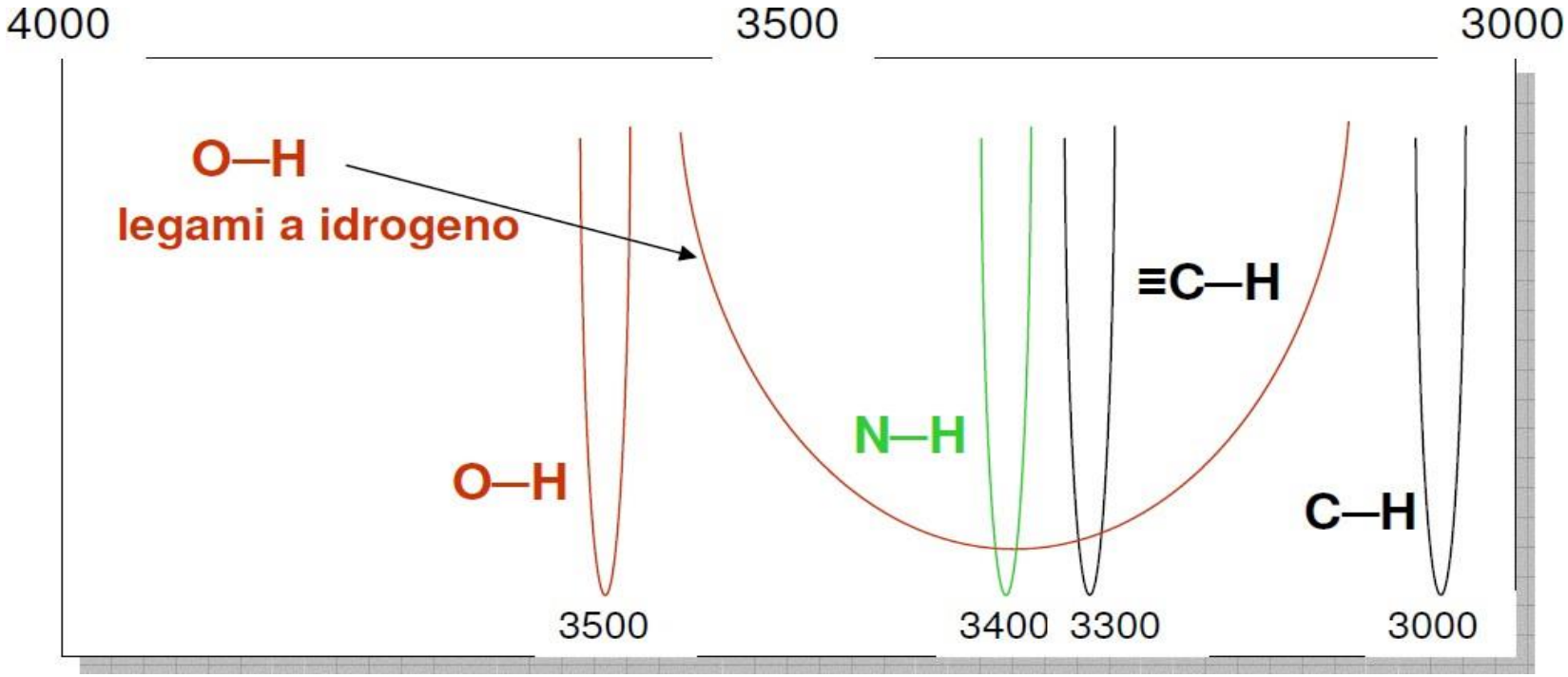

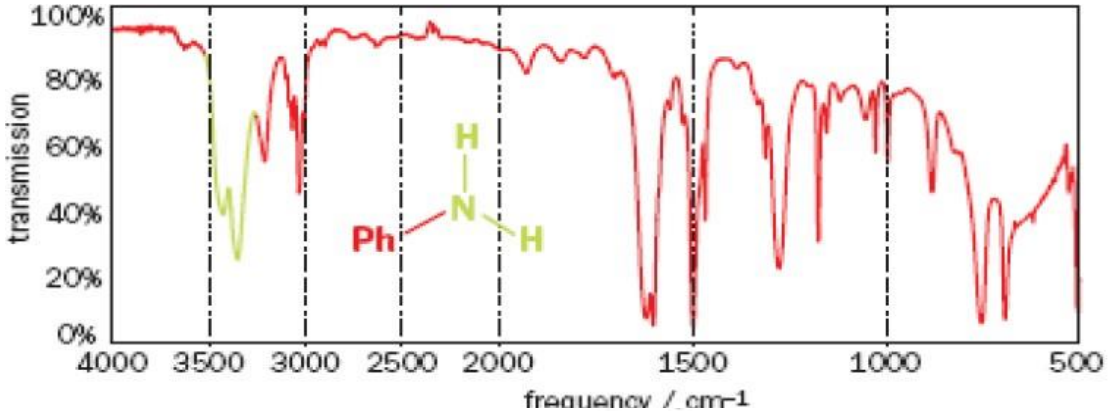

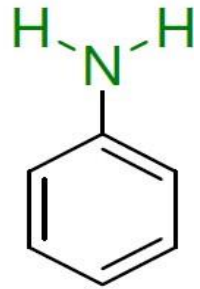

SIMMETRIC AND ASIMMETRIC STRETCHING

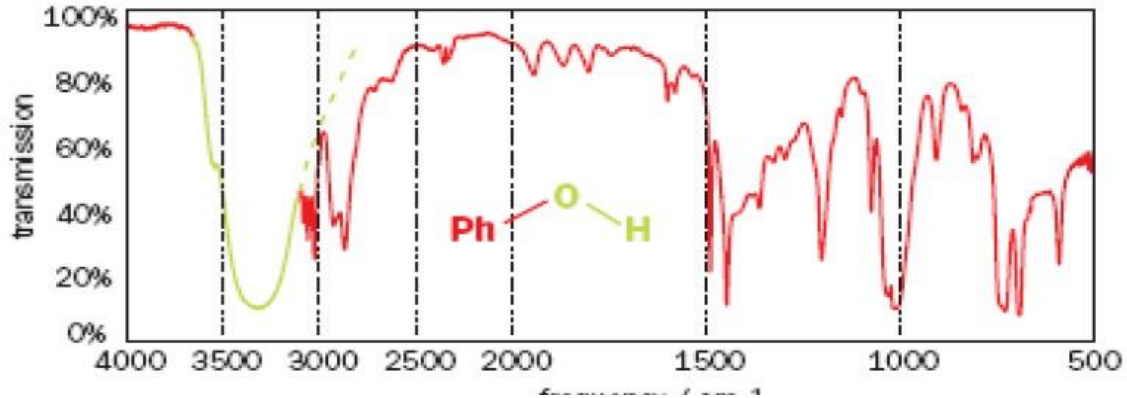

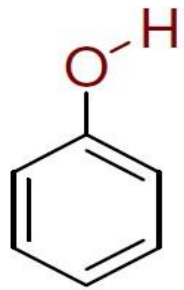

HYDROGEN BONDS

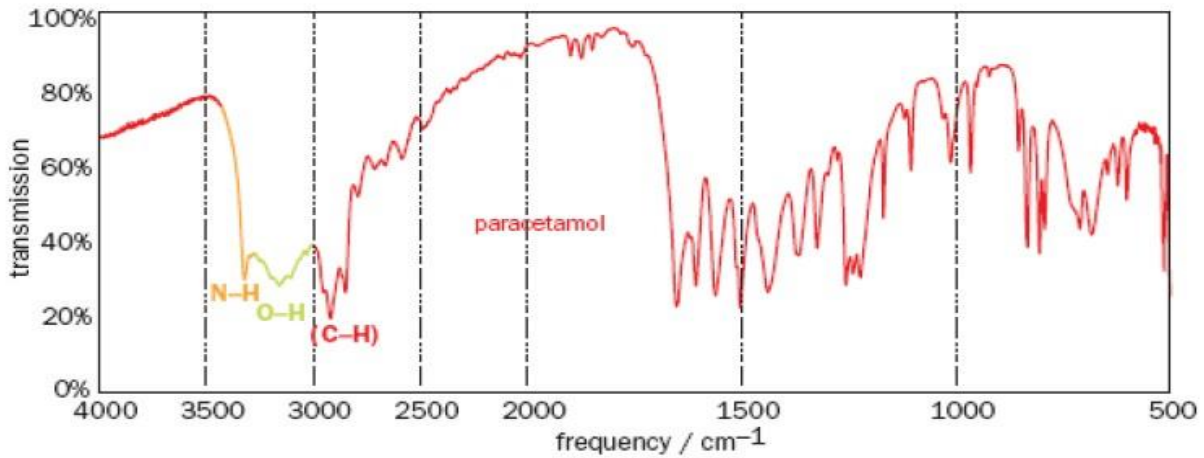

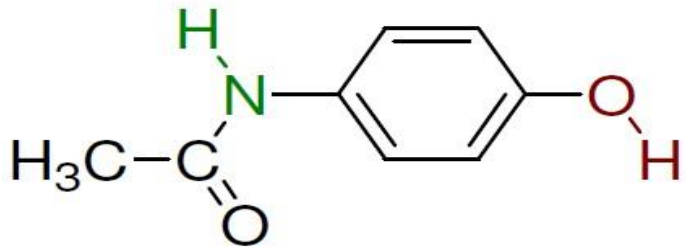

ANALYTICAL CHEMISTRY - INFRARED SPECTROSCOPY

Commonly referred to as IR spectroscopy, this technique allows chemists to identify characteristic groups of atoms (functional groups) present in molecules.

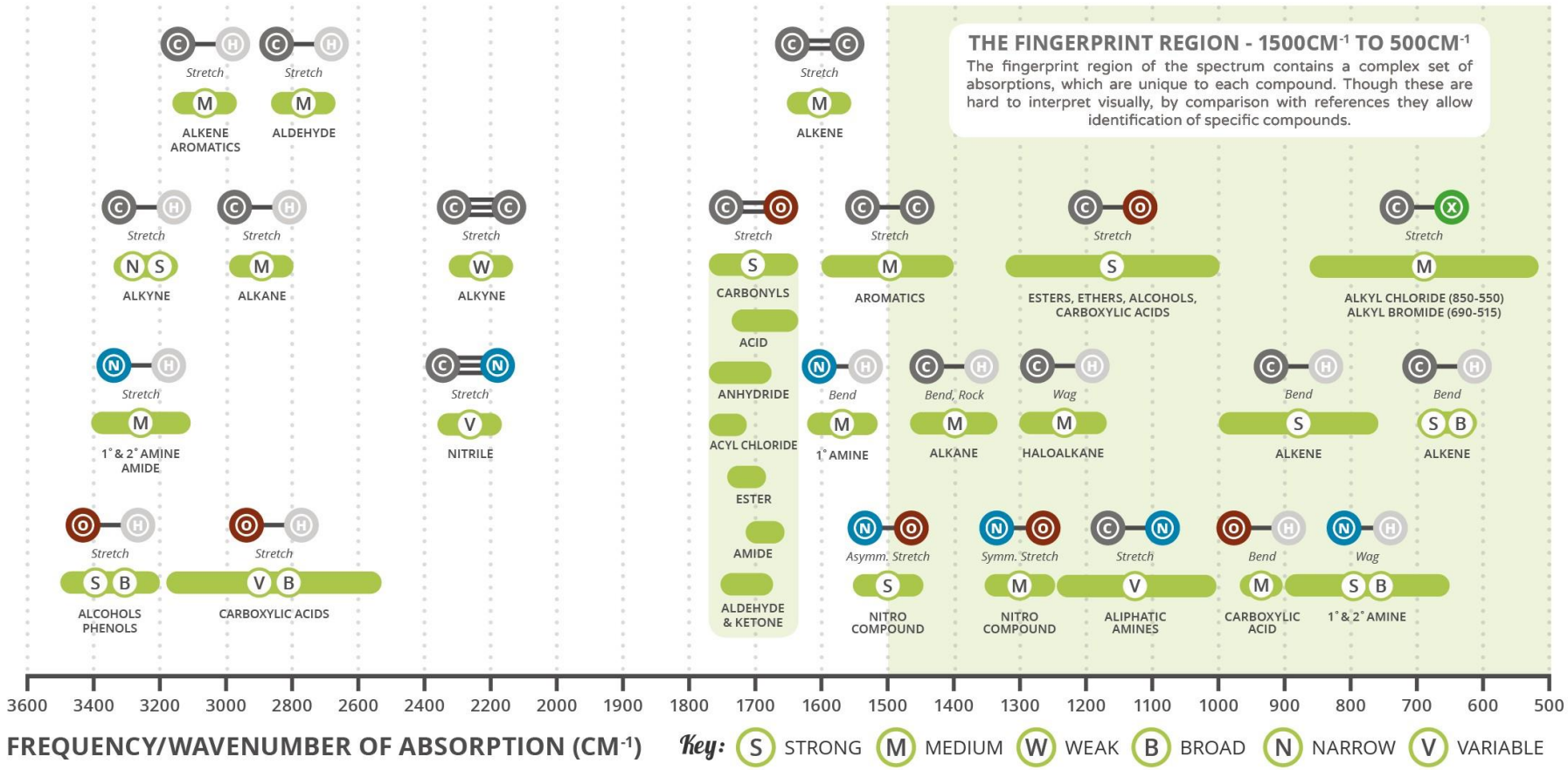

Infrared frequencies make up a portion of the electromagnetic spectrum. If a range of infrared frequencies are shone through an organic compound, some of the frequencies are absorbed by the chemical bonds within the compound. Different chemical bonds absorb different frequencies of infrared radiation. There are a number of characteristic absorptions which allow functional groups (the parts of a compound which give it its particular reactivity) to be identified. This graphic shows a number of these absorptions.

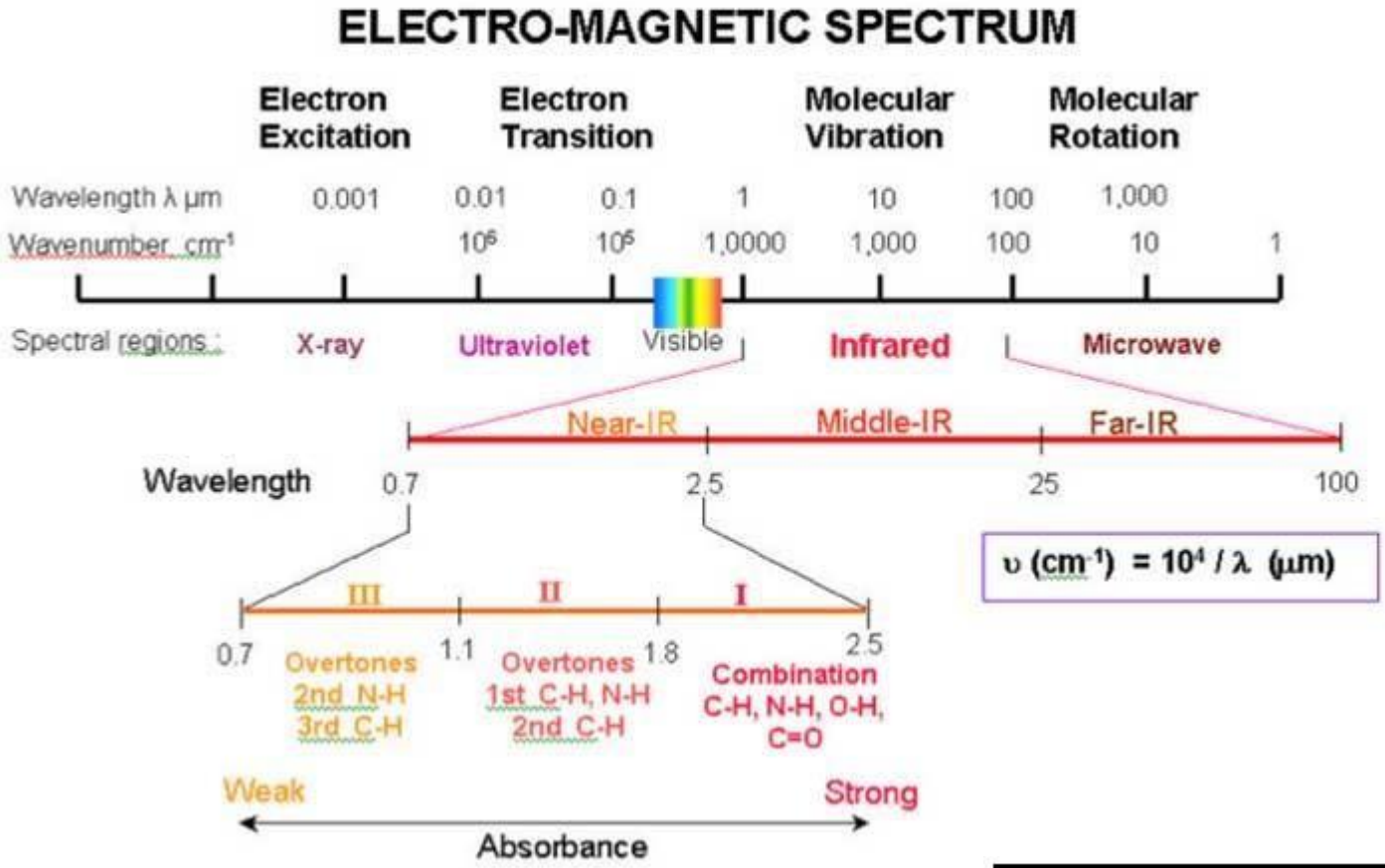
ELECTRO-MAGNETIC SPECTRUM
Electron Excitation
Electron Transition
Molecular Vibration
Molecular Rotation
Wavelength λ µm
0.001
0.01
0.1
1
10
100
1,000
Wavenumber, cm-1
10^6
10^5
1,0000
1,000
100
10
1
Spectral regions :
X-ray
Ultraviolet
Visible
Infrared
Microwave
Near-IR
Middle-IR
Far-IR
Wavelength
0.7
2.5
25
100
υ (cm-1) = 10^4 / λ (µm)
III
II
I
0.7
1.1
1.8
2.5
Overtones
2nd N-H
3rd C-H
Overtones
1st C-H, N-H
2nd C-H
Combination
C-H, N-H, O-H,
C=O
Weak
Strong
Absorbance

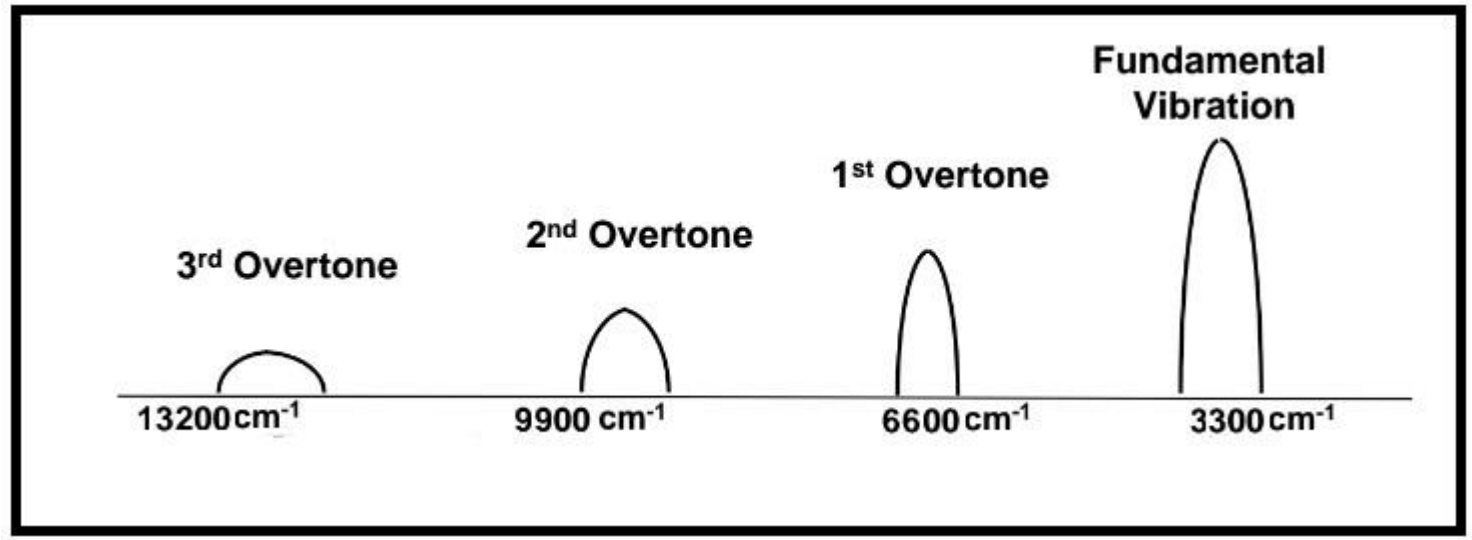
Fundamental Vibration
1st Overtone
2nd Overtone
3rd Overtone
13200 cm-1
9900 cm-1
6600 cm-1
3300 cm-1

SPETTROMETRI IR E FTIR (O FT-NIR)

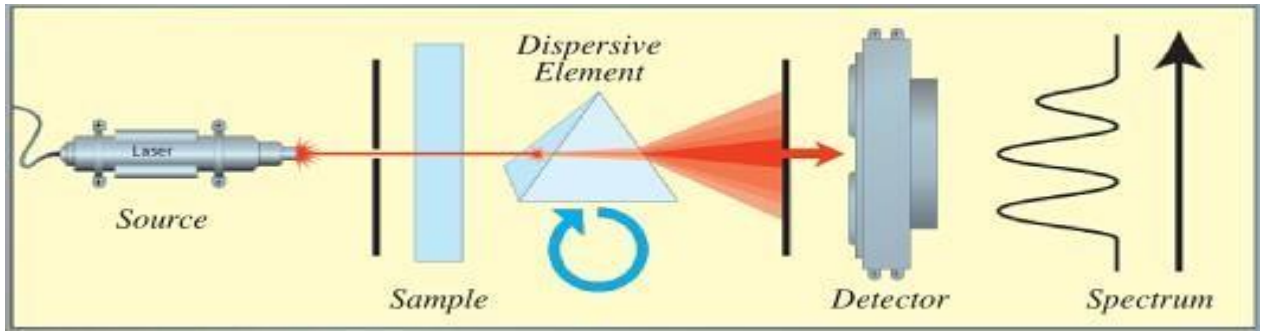

FT-IR

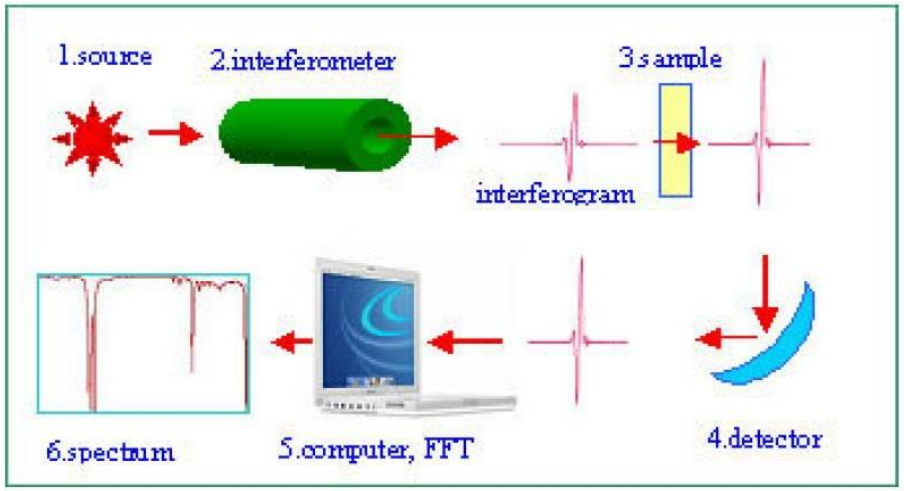

MICHELSON INTERFEROMETER

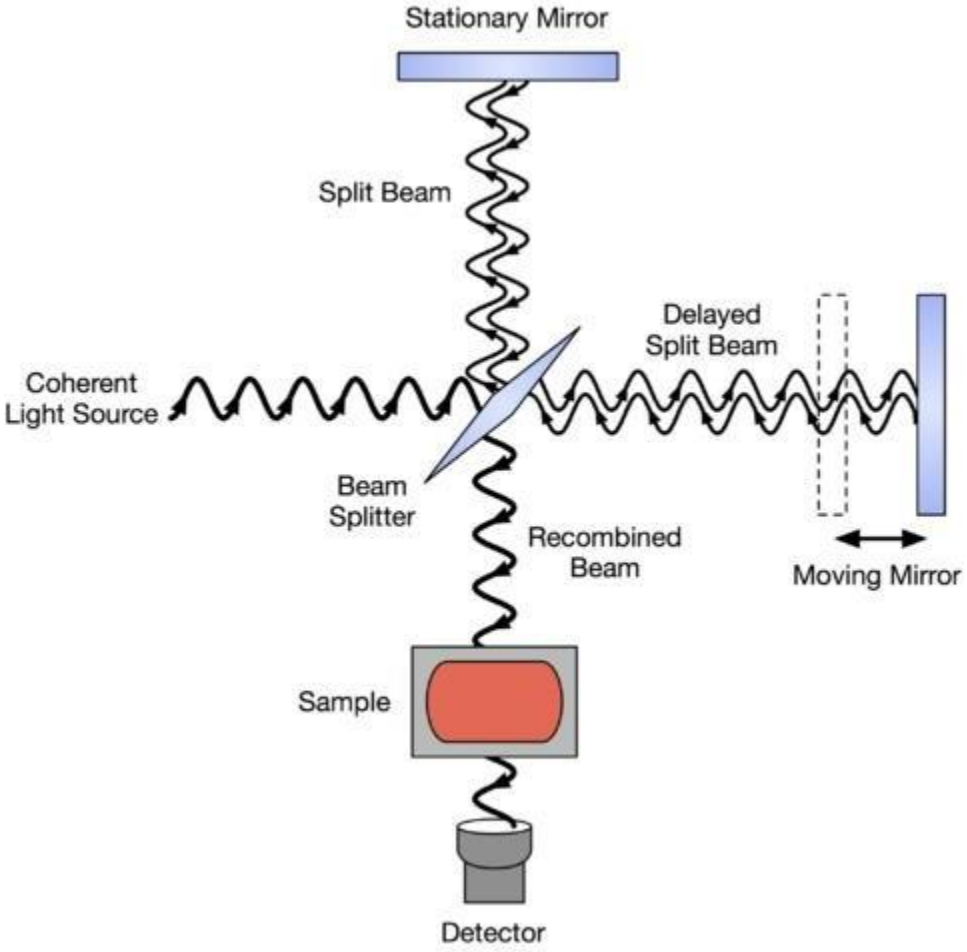

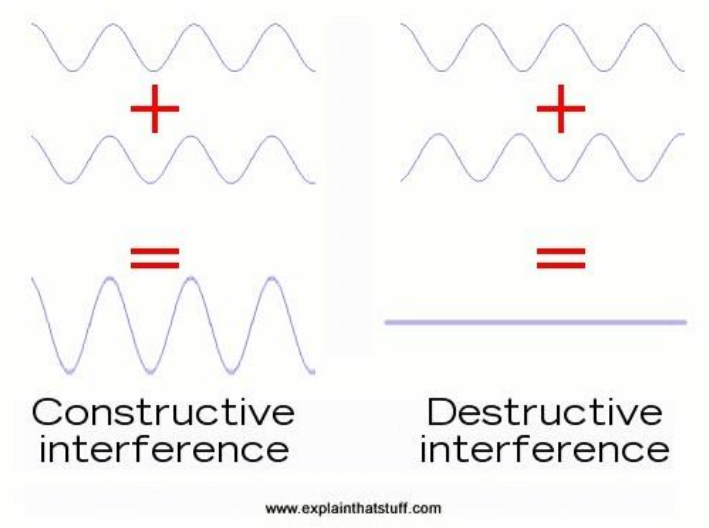

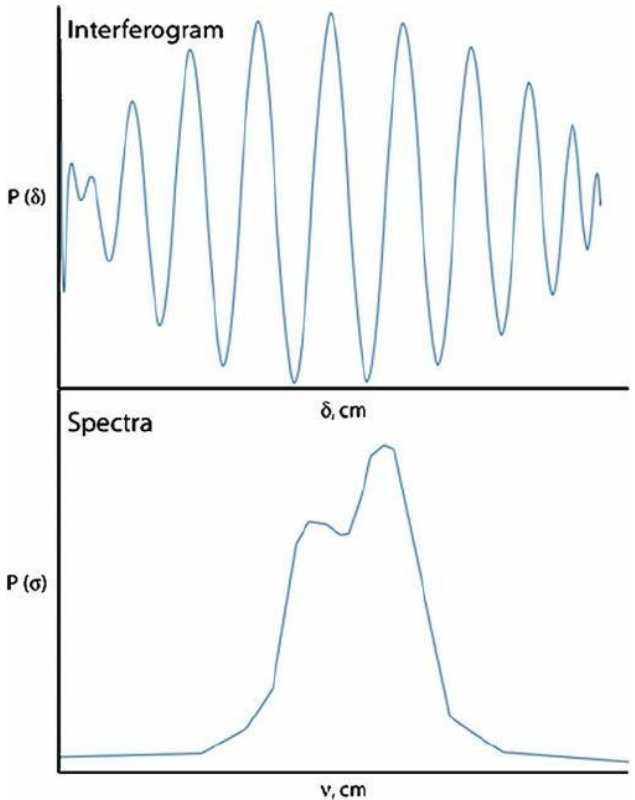

Light interference of multiple wavelengths(interferogram)

① monochromatic radiation of wavelengthλ

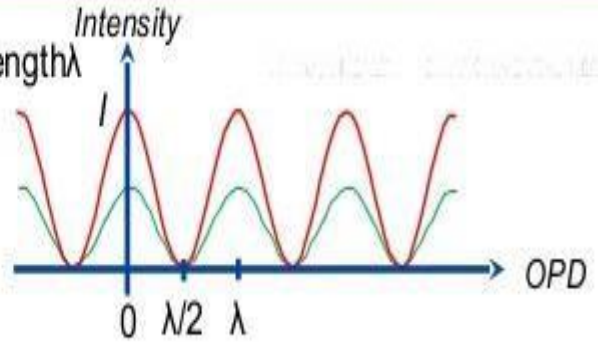

② two wavelengths radiation

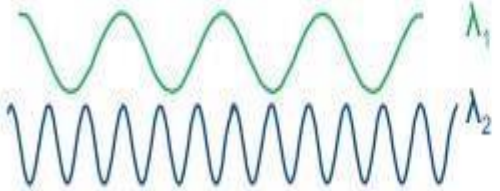

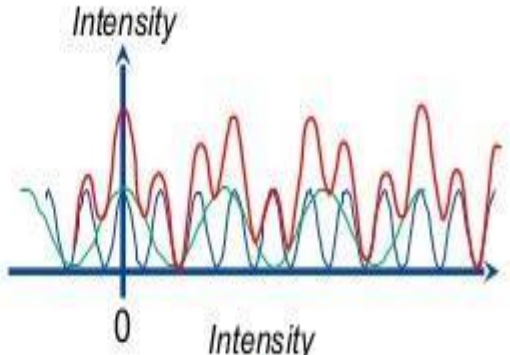

③ multiple wavelengths

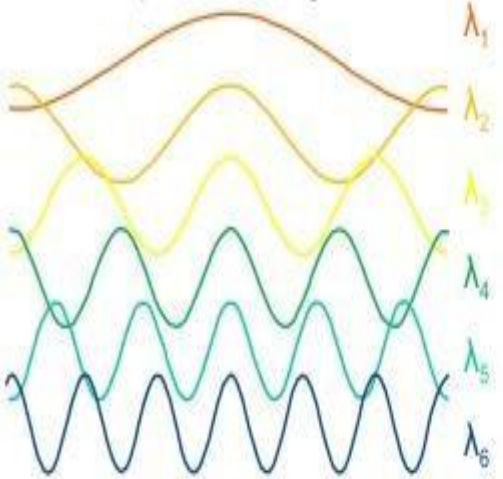

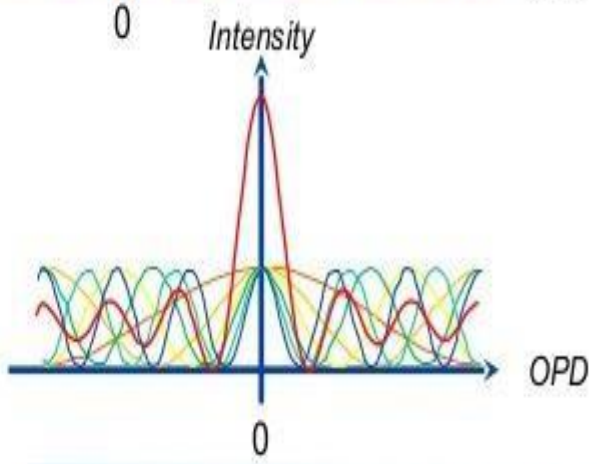

intensity is strongest at 0 optical path difference

Energy in infrared region and interferogram

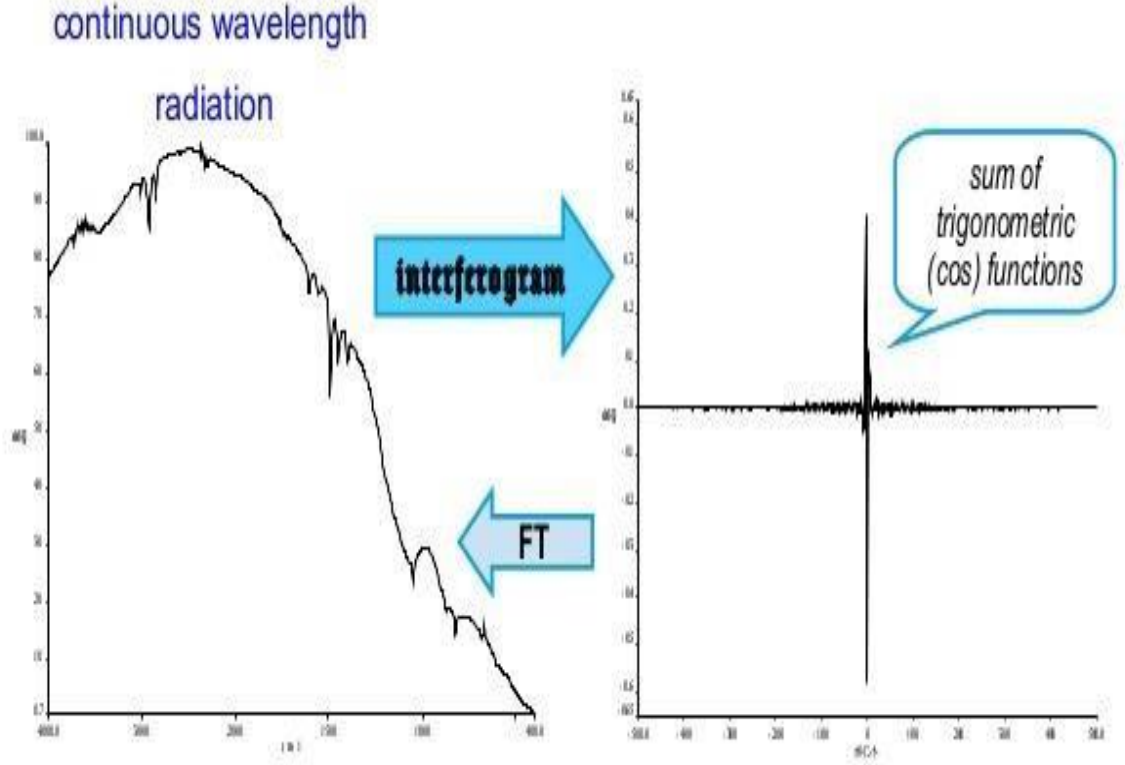

UNTREATED SAMPLES IN FTNIR

1. Attenuated Total Reflection

- The beam is directed onto optical dense crystal , *internal reflectance* create waves that extend to the sample in contact with crystal surface.

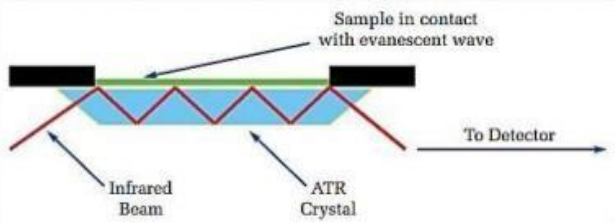

Analyze milk
using the Pearl FTIR

#SpectroscopyGuides

Quantitative analysis of :

- **Oleic acid**
- **Linoleic acid**
- **Saturated Fatty acids (SFA)**
- **Monounsaturated fatty acids (MUFA)**
- **Polyunsaturated fatty acids (PUFA)**
- **Peroxides value**

86 samples of extravirgin olive oil from Abruzzo, Marche e Puglia (2006 e 2007)

- **Chemical analysis (FA, PV, spectrophotometric indices)**
- **Determinaton of fatty acids (GC)**

FTIR spectra acquired with Tensor 27™ FTIR (Bruker Optics, Milan, Italy), inteferometer Rocksolid™ and detector DigiTect™ with ATR. ATR (Specac Inc., Woodstock, GA, USA) had ZnSe crystal.

Spectra (32 scans/sample) acquired in the 600 to 4000 cm^{-1} range with a resolution of 4 cm^{-1}.

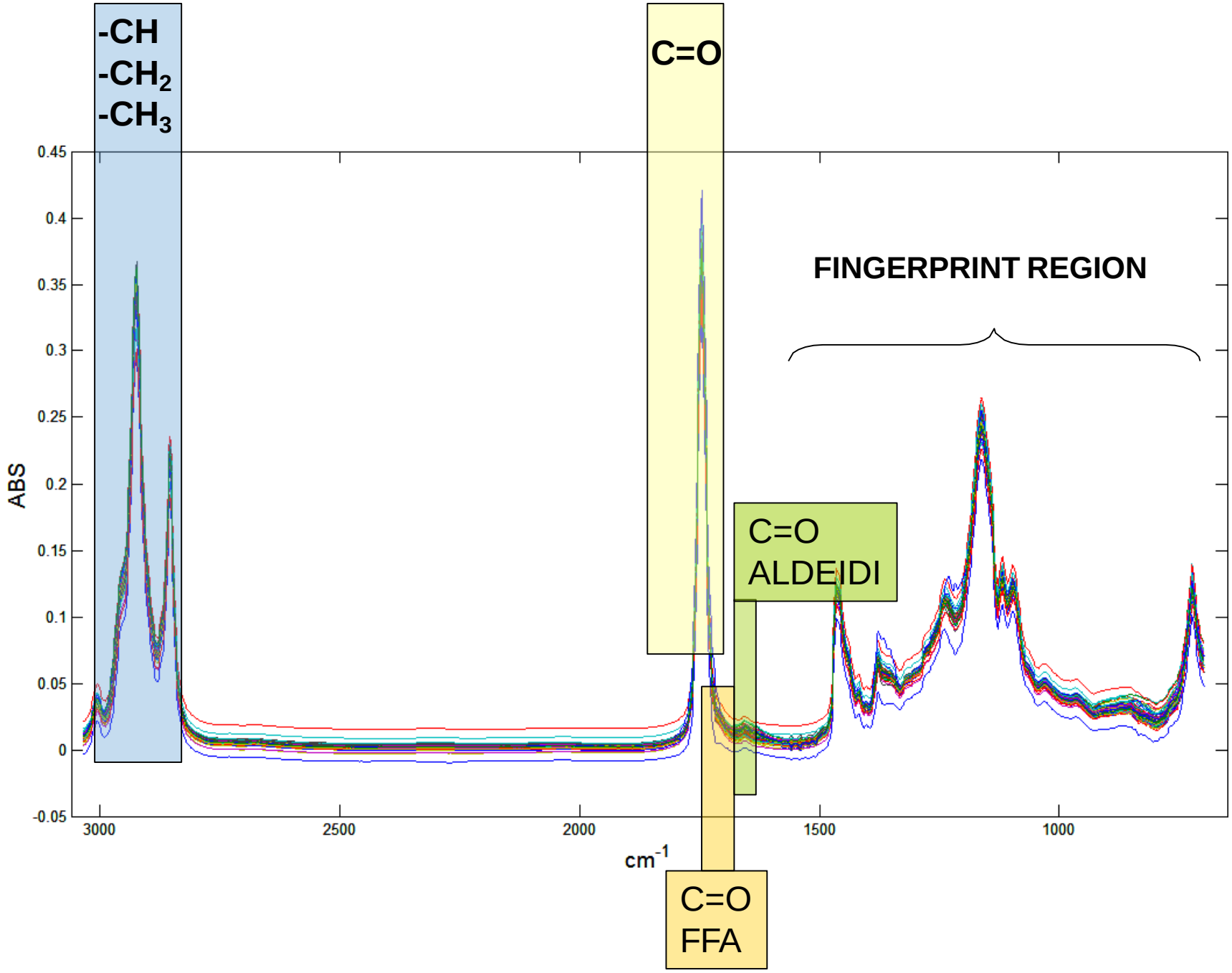
-CH
-CH2
-CH3
C=O
FINGERPRINT REGION
C=O
ALDEIDI
C=O
FFA
ABS
0.45
0.4
0.35
0.3
0.25
0.2
0.15
0.1
0.05
0
-0.05
3000
2500
2000
1500
1000
cm-1

Data processing and calibration models

Data exported as ASCII file with OPUS 6.0 software and processed with a PLS routine (Partial least squares) run on Matlab (Mathworks Inc., Natick, MA, USA).

For each parameter a PLS model has been built starting from a training set and taking as true value the data obtained using GC or chemical analysis

Spectra initially processed entirely have been reduced using a “moving-windows” strategy with a Matlab routine.

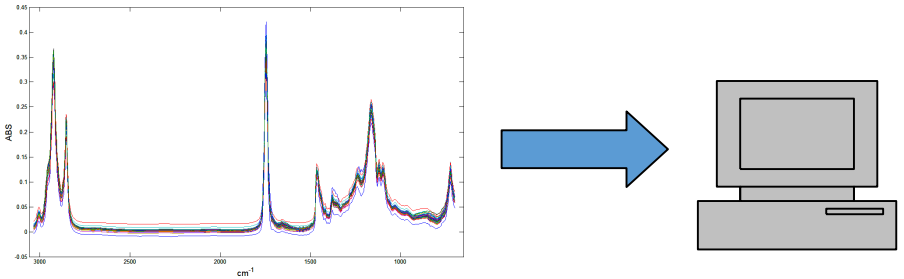

Property	MUFA	PUFA	SFA
Calibration			
Spectral range (cm^{-1})	700-3033	700-3033	700-3033
Linear range (% in VOO)	64 - 81	13 - 20	6 - 16
Number of factors (LVs)	14	15	13
Number of training samples (*N*)	61	61	61
PRESS[a]	10.59	2.52	6.11
Root mean square deviation (RMSD, %)	0.42	0.20	0.32
Relative error in calibration (REC %)	0.56	2.23	1.95
r^2	0.9883	0.9941	0.9557
Selectivity	0.1734	0.1988	0.1378
Sensitivity (SEN)	0.0009	0.0015	0.0020
Analytical sensitivity, [γ= (SEN/σ_0)]	0.17	2.07	0.32
Minimum concentration difference	6.0	0.48	3.17
Limit of detection (LOD, % in VOO)	3	0.28	1.3
Limit of quantification (LOQ, % in VOO)	10	0.94	4.5
Validation			
Number of validations samples	25	25	25
Recovery rates (%)	100	103	98
Relative error in Prediction, (REP, %)	1	4	6
r^2	0.8884	0.9816	0.7099
y_0	5 ± 5	0.4 ± 0.2	5 ± 1
Slope	0.93 ± 0.07	0.98 ± 0.03	0.7 ± 0.1

Results I: oleic and linoleic acid

Property	Oleic Acid	Linoleic Acid
Calibration		
Spectral range (cm^{-1})	700-3033	700-3033
Linear range (% in VOO)	62 - 80	5 - 15
Number of factors (LVs)	14	13
Number of training samples (*N*)	61	61
PRESS[a]	10.88	9.33
Root mean square deviation (RMSD)	0.42	0.39
Relative error in calibration (REC %)	0.51	4.64
r^2	0.9886	0.9773
Selectivity	0.1785	0.1988
Sensitivity (SEN)	0.0009	0.0016
Analytical sensitivity, [γ= (SEN/σ_o)]	0.18	1.17
Minimum difference (%)	5.6	0.9
Limit of detection (LOD, % in VOO)	3	0.5
Limit of quantification (LOQ, % in VOO)	10	1.7
Validation		
Number of validation samples	25	25
Recovery rates (%)	100	98
Relative error in Prediction (REP %)	1	7
r^2	0.9232	0.9444
y_o	4 ± 4	0.1 ± 0.4
Slope	0.94 ± 0.06	0.96 ± 0.05

Results II: MUFA, PUFA, SFA

Property	MUFA	PUFA	SFA
Calibration			
Spectral range (cm^{-1})	700-3033	700-3033	700-3033
Linear range (% in VOO)	64 - 81	13 - 20	6 - 16
Number of factors (LVs)	14	15	13
Number of training samples (*N*)	61	61	61
PRESS[a]	10.59	2.52	6.11
Root mean square deviation (RMSD, %)	0.42	0.20	0.32
Relative error in calibration (REC %)	0.56	2.23	1.95
r^2	0.9883	0.9941	0.9557
Selectivity	0.1734	0.1988	0.1378
Sensitivity (SEN)	0.0009	0.0015	0.0020
Analytical sensitivity, [γ= (SEN/σ_o)]	0.17	2.07	0.32
Minimum concentration difference	6.0	0.48	3.17
Limit of detection (LOD, % in VOO)	3	0.28	1.3
Limit of quantification (LOQ, % in VOO)	10	0.94	4.5
Validation			
Number of validations samples	25	25	25
Recovery rates (%)	100	103	98
Relative error in Prediction, (REP, %)	1	4	6
r^2	0.8884	0.9816	0.7099
y_o	5 ± 5	0.4 ± 0.2	5 ± 1
Slope	0.93 ± 0.07	0.98 ± 0.03	0.7 ± 0.1

Results III: PV

Property	D^o	D’	D”
Spectral range (cm^{-1})	4000-700	4000-700	4000-700
Calibration range ($meqO_2\ kg^{-1}oil$)	5.7-15.7	5.7-15.7	5.7-15.7
Number of factors (LV)	5	10	7
Number of training samples	23	24	24
PRESS[a] (unidades)	174.66	152.35	191.32
Root mean square deviation, RMSD (unidades)	1.4302	0.6933	0.9482
Relative error in calibration, REC (%)	15.6	7.2	9.9
r^2	0.8040	0.9759	0.9446
Selectivity	1.0	0.35	0.55
Sensitivity (SEN)	0.0044	0.0001	0.0001
Analytical sensitivity, [γ= (SEN/σ_o)]	1.2	1.1	1.1
Minimum concentration difference (unidades)	0.8	0.9	0.9
Limit of detection (LOD) (unidades)	3.1	1.0	1.6
Limit of quantification (LOQ) (unidades)	10.3	3.4	5.2
Number of validations samples	10	10	10
Recovery rates (%)	74.7	97.7	96.0
Relative error in Prediction, REP (%)	23.7	13.6	12.2

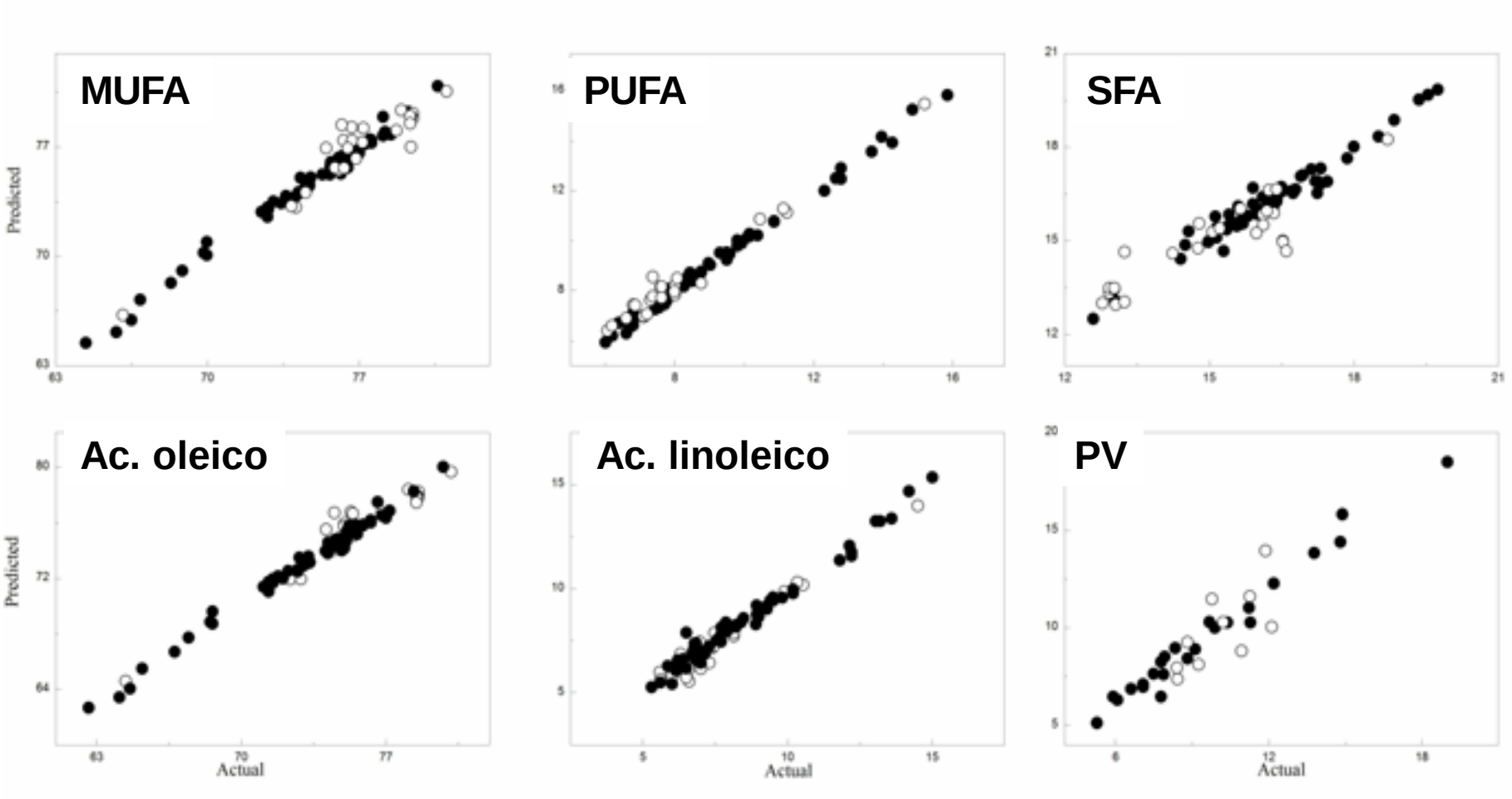

calibration set (●) and trainingset (○)

Analytical and Bioanalytical Chemistry (2020) 412:1077–1086
https://doi.org/10.1007/s00216-019-02332-w

RESEARCH PAPER

Spectrochemical differentiation of meningioma tumours based on attenuated total reflection Fourier-transform infrared (ATR-FTIR) spectroscopy

Taha Lilo[1,2] · Camilo L. M. Morais[2] · Katherine M. Ashton[3] · Ana Pardilho[1] · Charles Davis[2] · Timothy P. Dawson[3] · Nihal Gurusinghe[1] · Francis L. Martin[2]

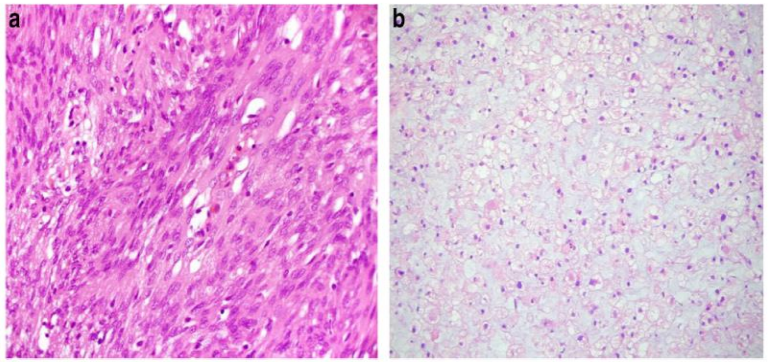

Fig. 1 H&E slides. (**a**) WHO grade I meningioma (transitional meningioma). (**b**) WHO grade II meningioma (clear cell)

Table 3 Quality metrics for PCA-LDA and PLS-DA models to distinguish grade I vs. grade I recurrence samples

Algorithm	Dataset	Accuracy (%)	Sensitivity (%)	Specificity (%)
PCA-LDA	Training	95	99	34
	Validation	95	99	32
PLS-DA	Training	96	96	100
	Validation	94	94	94

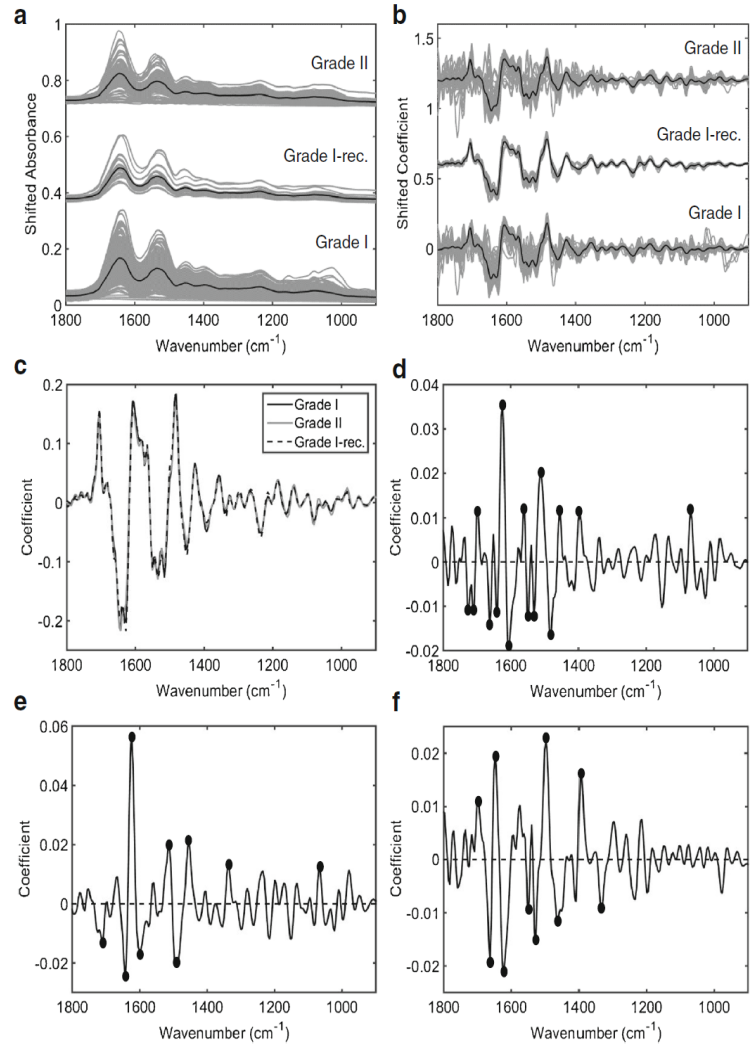

Fig. 2 Infrared spectra for meningioma tumour samples (grade I, grade I recurrence and grade II). (**a**) Raw spectra and (**b**) pre-processed spectra (Savitzky-Golay 2nd derivative and vector normalisation), where black line represents mean spectrum. (**c**) Mean spectrum for each class overlaid. (**d**) Difference-between-mean (DBM) spectrum for grade II (+) vs. grade I (−) meningiomas. (**e**) DBM spectrum for grade II (+) vs. grade I recurrence (−) meningiomas. (**f**) DBM spectrum for grade I recurrence (+) vs. grade I (−) meningiomas, where solid dots represent spectral wavenumbers with absolute coefficients > 0.01

Cancer Letters 477 (2020) 122–130

Contents lists available at ScienceDirect

Cancer Letters

journal homepage: www.elsevier.com/locate/canlet

Mini-review

Biofluid diagnostics by FTIR spectroscopy: A platform technology for cancer detection

Alexandra Sala[a], David J. Anderson[a], Paul M. Brennan[b], Holly J. Butler[c], James M. Cameron[a], Michael D. Jenkinson[d], Christopher Rinaldi[a], Ashton G. Theakstone[a], Matthew J. Baker[a,c,*]

[a] WestCHEM, Department of Pure and Applied Chemistry, University of Strathclyde, Technology and Innovation Centre, 99 George Street, Glasgow, G1 1RD, UK
[b] Translational Neurosurgery, Department of Clinical Neurosciences, Western General Hospital, Edinburgh, EH4 2XU, UK
[c] ClinSpec Diagnostics Ltd., Technology and Innovation Centre, 99 George Street, Glasgow, G1 1RD, UK
[d] Institute of Translational Medicine, University of Liverpool & the Walton Centre NHS Foundation Trust, Lower Lane, Fazakerley, Liverpool, L9 7LJ, UK

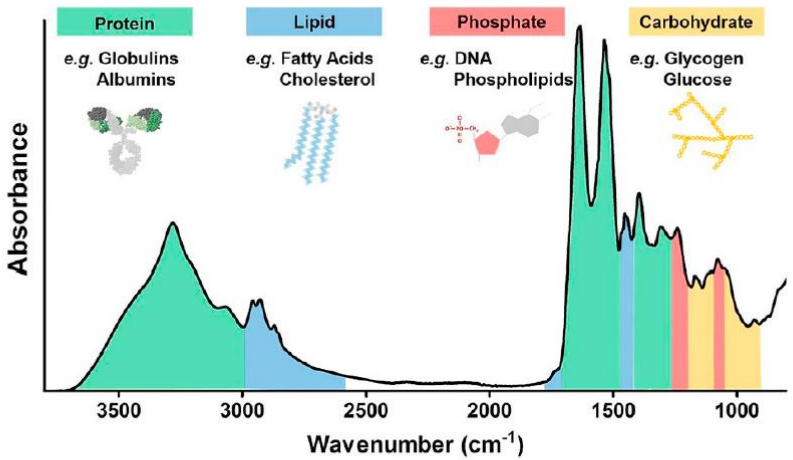

Fig. 2. Human blood serum spectrum acquired by ATR-FTIR spectroscopy with relative biomolecules associated to peaks. Adapted with permission from Ref. [22].

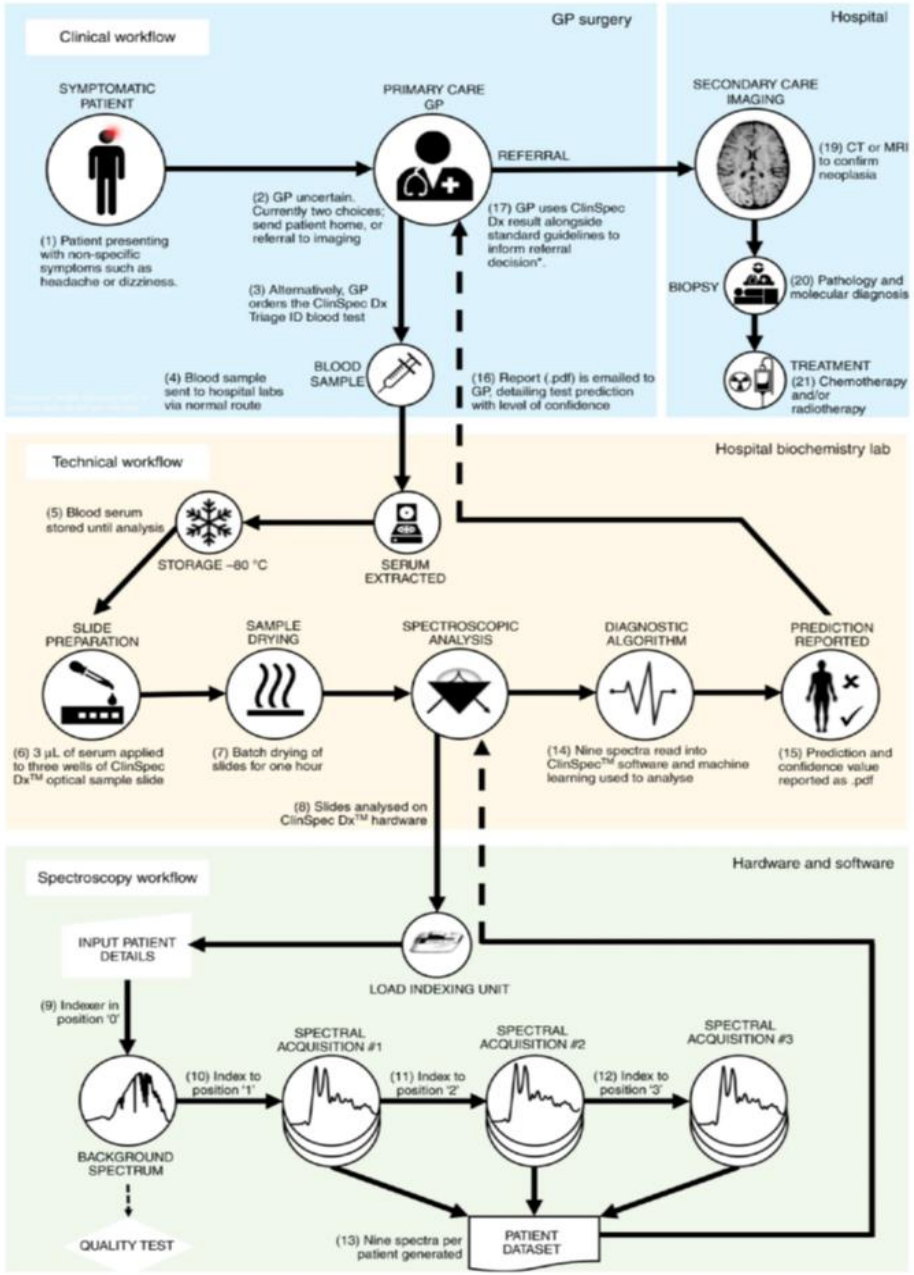

Fig. 3. Proposed integration of a blood test for the triage of brain cancer. Reproduced from Ref. [31] (CC by 4.0).